8-7-2008

Nonaqueous Synthesis of Metal Oxide Nanoparticles and Their Surface Coating

Ming Zhang
University of New Orleans

Nonaqueous Synthesis of Metal Oxide Nanoparticles and Their Surface Coating

A Dissertation

Submitted to the Graduate Faculty of the
University of New Orleans
in partial fulfillment of the
requirements for the degree of

Doctor of Philosophy
in
The Department of Chemistry

By

Ming Zhang

B.E. University of Science and Technology of China, 2002

B.S. University of Science and Technology of China, 2002

August 2008

Acknowledgments

I would like to express my gratitude to my adviser, Professor Charles O'Connor. He guided me through my six years of work. Many thanks for his patience, confidence and the opportunity he offered for me to gain professional experience and maturity.

I would like to thank my committee members Professor John Wiley, Professor Kevin Stokes, Professor Weilie Zhou and Professor Ferdinard Poudeu. They gave me suggestions and fresh ideas in many valuable discussions.

I would also like to thank Dr Tarr, Dr. Sweany and Dr. Spinu for their great help in my research work. They made a great effort to make all my intended measurements possible. I must thank all my coworkers and friends for sharing their knowledge and experience with me. Not only did I learn a lot from them but I found my work much easier with their help.

Last, but not the least, I would like to thank my wife, Lifang Shi and my parents, who gives me encourage and support all the time.

The dissertation is also for my beloved baby boy Lucas.

TABLE OF CONTENTS

LIST OF FIGURES

ABSTRACT

This thesis mainly consists of two parts, the synthesis of several kinds of technologically interesting crystalline metal oxide nanoparticles via high temperature nonaqueous solution processes and the formation of core-shell structure metal oxide composites using some of these nanoparticles as the core with silica, titania or polymer as shell via a modified microemulsion approach.

In the first part, the experimental procedures and characterization results of successful synthesis of crystalline iron oxide (Fe_3O_4) and indium oxide (In_2O_3) nanoparticles are reported. Those nanoparticles exhibit monodispersed particle size, high crystallinity and high dispersibility in non-polar solvents. The particle size can be tuned by the seed mediated growth and the particle shape can also be controlled by altering the capping ligand type and amount. The mixed bi-metal oxides such as cobalt iron oxide and lithium cobalt oxide will be discussed as well.

In the second part, the synthesis and characterization of various surface coated metal oxides, including silica, titania and polymer coated nanocomposites are reported. The silica coating process is presented as a highlight of this part. By using a microemulsion system, core-shell structure silica coated iron oxide and indium oxide nanocomposites are successfully prepared. Furthermore, the thickness of the silica coating can be controlled from 2 nm to about 100 nm by adjusting the reaction agents of the micelle system. By extending the procedure, we will also discuss the titania and polymer coating preparation and characterization.

Keywords: magnetic nanoparticles; semiconductor nanoparticles; silica; polymer; coating.

Chapter 1 Introduction

1.1 Nanoscience and nanotechnology

In the past few decades, a small word attracted enormous attention, interest and investigation around the world: "***nano***". What it presents in terms of science and technology, which are also called nanoscience and nanotechnology, is much, much more than just a word describing a specific length scale. It has dramatically changed every aspect of the way that we think in science and technology and will definitely bring more and more surprises into our daily life as well as into the world in the future.[1-8]

What is actually so exciting about "nano"? "Nano" means one billionth (10^{-9}), so 1 nanometer refers to 10^{-9} meter and is expressed as 1 nm. 1 nm is so small that things smaller than it can only be molecules, clusters of atoms or particles in the quantum world. The nanometer is a special point in the overall length scale because nanometer scale is the junction where the smallest manufacture objects "meet" the largest molecules in nature. The structures, devices and systems having at least one dimension in nanometer scale are not only smaller than anything that we've ever made before, but also possibly the smallest solid materials that we are able to produce. Besides, in nanometer scale, the properties of materials that we are familiar with in our daily life, such as color, melting point, electronic, catalytic or magnetic properties, will change dramatically or be replaced by completely novel properties due to what is usually called size effect. "At this size scale, everything, regardless of what it is, has new properties. And that is, where a lot of

the scientific interest is." said Professor Alivisatos. This is just the beginning of what make "nano" so interesting.[9-12]

What are nanoscience and nanotechnology? In fact, there are no exact definitions for them. The following is the definition of nanoscience and nanotechnology given by the U.S. National Nanotechnology Initiative (NNI): nanoscience and nanotechnology are "Research and technology development at the atomic, molecular and macromolecular levels in the length scale of approximately the 1-100 nanometer range, to provide a fundamental understanding of phenomena and materials at the nanoscale and to create and use structures, devices and systems that have novel properties and functions because of their small and/or intermediate size". Simply saying, nanoscience tells us how to understand the basic theories and principles of nanoscale structures, devices and systems (1-100 nm); and nanotechnology tells us what to do and how to use these nanoscale materials. [13,14]

On December 29, 1959, Nobel Prize winner, physicist Richard P. Feynman said in his famous speech "There is Plenty of Room at the Bottom": "In the year 2000, when they look back at this age, they will wonder why it was not until the year 1960 that anybody began seriously to move in this (nanometer) direction." Actually, in the years after, people did want to "move in this direction". However, not much progress was made in both nanoscience and nanotechnology until the 1980's when scanning tunneling microscope (STM) and other advanced analytical measurements were invented because there were not many suitable analytical tools available to investigate nanometer scale

materials. After STM, TEM, SEM and AFM, highly advanced analytical tools were developed (and are still developed) rapidly, which enables the characterization and manipulation of small objects down to a few nm bringing a human being's view into real atomic world. As one of the consequences of explosive development of nanoscience, nanotechnology had its breakthrough before the coming of the new century. Nowadays, many remarkable techniques, such as nanoimprint lithography, self-assembly technique, nanoscale crystal growth technique, are already available to make nanoscale products in relatively large amounts, showing the great potentials of nanotechnology in real applications. [15-20]

Although the term of nanomaterials represents a large variety of materials in the domain of nanometers, nanoparticles have been always considered as one of a few core materials in nanoscience and nanotechnology. The reasons are, in addition to the size effect, nanoparticles represent the most popular morphology of the nano-scale world and are ideal manipulative building blocks to construct larger devices, structures and systems following the so-called "bottom-up" approach in nanotechnology. Many discoveries related to nanoparticles synthesis, such as the discovery of ferrite particles, the synthesis of well-defined quantum dots or the shape control of CdSe nanocrystals, can be regarded as milestones in the history of nanoscience, which further proves the important role of nanoparticles in nanoscience.

Nowadays, the synthesis, characterization and application of nanoparticles represent a highly dynamic area in both the scientific research and business communities.

Definitely, the synthesis of nanoparticles is the crucial step in this area. Human beings started synthesizing and utilizing nanoparticles more than one thousand years ago. The ancient Chinese used carbon nanoparticles to produce the famous and superfine Hui Ink for handwritings and paintings; they still keep their fresh color after thousand years. Roman glassmakers used noble metal nanoparticles to fabricate colored glasses as early as in the fourth century A. D. Real scientific research on nanoparticles was started in the mid-nineteenth century and didn't experienced tremendous development until the last decades. Today, there is a huge toolbox available to successfully synthesize both organic and inorganic nanoparticles using greatly diverse approaches. For instance, liquid-phase techniques, including coprecipitation, sol-gel chemistry, microemulsion, hydrothermal/solvothermal processing and template syntheses, are particularly useful for the synthesis of inorganic particles based on its ability of synthesizing broad classes of nanoparticles and controlling particle size and morphology.[21-25]

Among the various classes of inorganic nanoparticles, metal oxide nanoparticles are particularly attractive from both the scientific and technological point of view. The unique characteristics of metal oxides make them the most diverse class of materials, with optical, electronic, electrical, photoelectronic, catalytic or magnetic properties covering almost all aspects of materials science and solid state physics. When metal oxides are brought into the nanometer scale, they further exhibit improved or completely novel properties compared to their bulk materials. Their fascinating properties certainly enable their various applications in nanotechnology, such as in gas sensing, bio-applications, catalysis, superconductors and energy conversions, and so on.

1.2 Methods for producing nanomaterials[26-42]

The interest in nanoscale objects is due to the exhibition of novel electronic, optical, magnetic, transport, photochemical, electrochemical, catalytic, mechanical, biological and medical properties and behaviors, depending on composition, size, and shape of the nanoproducts. In fact, many interesting phenomena at the nanoscale are caused by the tiny size of the organized structure and by interactions at their predominant and complex interfaces, which is different than with the bulk materials. It is believed that when chemists are able to gain control over size and shape of the particles, further enhancement of material properties and device functions will surely be possible. Most of the discovered new materials and new physical or chemical properties are due to the change in both, composition or size.

As a result, the new applications and properties are rather a result of tailoring matter and subsequently arranging the components by means of chemical interactions, so, ideally, new properties can arise from a combination of inexpensive and environmentally harmless components. But the chemist not only has to be able to synthesize perfect, monodispersed and shape-defined objects having nanometer dimensions, but they also could have to position these objects in appropriately organized arrays. This could be tackled either by using lithographic techniques or templating methods (molecular and supramolecular assembly processes, or deposition inside the void spaces of nanoporous host materials).

Before working with nanoparticles, it is first necessary to be able to produce them. At present, most of the nanochemistry is concerned with the development of novel methods for the synthesis and characterization of chemical systems within the size range of about 1 to 100 nm and their applications. Generally, there are two methods for producing nanomaterials. One method is to generate particles of the correct size using crystallization, direct generation or other similar techniques, which is often referred to as "bottom up." In the other method, referred to as "top down," larger particles are reduced through milling to achieve the desired nanoscale particles.

Current fabrication technology for nanoparticles is novel and versatile. Significant progress has been made over the last decade in understanding fundamental aspects of the synthesis of nanoparticles, nanorods. Various processing routes have been developed for the synthesis and commercial production of nanoparticles including vapor, liquid, solid state processing routes, and combined methods, such as the vapor–solid–liquid approach.

Available techniques for the synthesis of nanoparticles via vapor routes range from physical vapor deposition (PVD) and chemical vapor deposition (CVD) to aerosol spraying. The liquid route involves sol–gel and other wet chemical methods. Solid state route preparations take place via mechanical milling and mechanochemical synthesis. Each method has its own advantages and disadvantages. Different synthesis routes would give us different internal structures of nanoproducts that would affect the properties of materials consolidated from them. Due to their high specific surface areas, nanoparticles exhibit a high reactivity and strong tendency towards agglomeration. Moreover, rapid

grain growth is likely to occur during processing at high temperatures. As unique properties of nanocrystaline materials are derived from their fine grain size, it is of crucial importance to retain the microstructure at a nanometer scale during consolidation to form bulk materials. It is also apparent that pores are generated in bulk nanocrystalline materials consolidated from nanoparticles prepared by inert-gas condensation. Electrodeposited samples are believed to be free from porosity, but they contain certain impurities and texture that may degrade their mechanical performances. Therefore, controlling these properties during synthesis and subsequent consolidation procedures are the largest challenges facing researchers today.

Comprehensive understanding of the processing-structure-property relationships is essential in the development of novel nanomaterials with unique properties for structural engineering applications.

1.2.1 Vapor route

1.2.1.1 Physical vapor deposition

Physical vapor deposition (PVD) is a versatile synthesis method and is capable of preparing thin film materials with structural control at the atomic or nanometer scale with careful monitoring of the processing conditions. PVD involves the generation of vapor phase species either via evaporation, sputtering, laser ablation or ion beam deposition. Inert gas condensation combined with thermal evaporation is commonly used to fabricate

metallic and metal-oxide powders with a well defined and narrow size distribution. This technique was originally introduced by Ganqvist and Buhrman in 1976 and developed by Gleiter in 1981.

1.2.1.2 Chemical vapor deposition

Chemical vapor deposition (CVD) is a process where one or more gaseous adsorption species react or decompose on a hot surface to form stable solid products. Otherwise, the fundamental theory of CVD is similar to PVD .

1.2.1.3 Spray conversion processing

This route involves the atomization of chemical precursors into aerosol droplets that are dispersed throughout a gas medium. The aerosols are then transported into a heated reactor where the solution is evaporated or combusted to form ultrafine particles or thin films. This technique is versatile and inexpensive because of the availability of various low cost chemical solutions and has been used to produce a variety of high purity and non-agglomerated metal oxide nanoparticles such as TiO_2, Al_2O_3, ZrO_2, V_2O_5 and Y_2O_3–ZrO_2.

1.2.2 Liquid route

1.2.2.1 Sol–gel process

Sol–gel processing is particularly attractive because the chemical reactions can be tailored at the molecular level. Using molecular precursors to obtain an oxide or hydroxide network via hydrolysis and condensation reactions, sol–gel process provides new approaches and a better control in the preparation of nanomaterials. However, the alkoxides used are rather expensive, and the processing is tedious because it requires several sequential steps to form nanoparticles or nanocrystalline solids. The sol–gel processing method has been used for producing metal oxide and ceramic powders with high purity and high homogeneity for many years. The sol–gel route offers a degree of control of composition and structure at the molecular level. The process involves the generation of a colloidal suspension (‘sols’) which are subsequently converted to viscous gels and solid materials. Ebelman produced the first silica gels in 1846 and Cossa synthesized alumina gels in 1870. Since then, aerogels of zirconia, silazane, borate and other ceramics were synthesized using the sol–gel technique. In the process, reactive metal precursors were initially hydrolyzed, followed by condensation and polymerization reactions. Metal alkoxides are metal organic compounds having an organic ligand attached to a metal or metalloid atom. They are the result of direct or indirect reactions between a metal M and an alcohol ROH. Typical examples are methoxide (OMe; $MOCH_3$) and ethoxide (OEt; MOC_2H_5). During hydrolysis, the alkoxy groups (OR) are replaced by hydroxo ligands.

1.2.2.2 Wet chemical synthesis

Solution-based processing routes used for the synthesis of nanoparticles include precipitation of solids from a supersaturated solution, homogeneous liquid phase chemical reduction, microemulsions, hydrothermal/solvothemal processing of nanoparticles and nanocomposites, and ultrasonic decomposition of chemical precursors. These processes are attractive due to their simplicity, versatility and availability of low cost precursors. Inorganic salt compounds used in the wet chemical synthesis routes are more versatile and economical than alkoxides employed in the sol–gel process. A typical example is the formation of nanocrytalline titania powders via hydrolysis of $TiCl_4$ at lower temperatures:

$$TiCl_4+2H_2O \rightarrow TiO_2+4HCl$$

Salt reduction is one of the most commonly adopted methods to generate the metal colloid particles. The process involves the dissolution of metal salts in aqueous or non-aqueous environments followed by the reduction of metal cations to the zero-valent state. The nature of the metal salts determines the kind of reducing agent to be applied. To produce transition metal nanoparticles, metal chlorides such as $CrCl_3$, $MoCl_3$ and WCl_4 are reduced with $NaBH_4$ solution at room temperature to form metal colloids of high yield.

Microemulsion synthetic methods can be used for synthesis of metals or alloys by reduction, and synthesis of metal oxides or other inorganic nanomaterials which we will

discuss in the later chapters. In a sealed vessel (bomb, autoclave, *etc*.), solvents can be brought to temperatures well above their boiling points by the increase in autogenous pressures resulting from heating. Performing a chemical reaction under such conditions is referred to as *solvothermal processing* or, in the case of water as solvent, *hydrothermal processing*. More recently, Cheng and co-workers[34] developed a method for preparing nanoparticulate, phase-pure rutile and anatase from aqueous $TiCl_4$ by a hydrothermal process. This method has become one of the most important techniques for preparation of nanomaterials.

Metal and metal oxide nanoparticles can also be generated via ultrasonic and thermal decomposition of metal salts or chemical precursors. Recently, ultrasonic waves have been employed to stimulate the chemical reaction of inorganic salts.

Our works are mainly based on wet chemistry technique including high temperature solution phase synthesis for nanoparticles production and microemulsion method for nanoparticles modification.

1.2.3 Solid route

1.2.3.1 Mechanical alloying/milling

The mechanical alloying/milling process is a solid state processing technique and was originally developed by Benjamin of the International Nickel Company for the production of oxide dispersion strengthened (ODS) super alloys. In this process, high energy ball milling is used for synthesizing a variety of materials like forming

equilibrium and non-equilibrium phases. The mechanical energy transfer to the powder particles in these mills takes place by shear action or impact of the high velocity balls with the powder. During the process, raw powder particles with a size of several microns experience severe plastic deformation undergo a repetitive cold welding and fracturing mechanism60. Vibratory mill, planetary mill, uniball mill and attritor mill are commonly used to perform mechanical alloying/milling. Due to mechanical limitations, these methods cannot produce very small particles. However, the advantage of this method is its relative simplicity, low cost, and the possibility to scale it to tonnage quantities.

1.2.3.2 Mechanochemical synthesis

This process involves mechanical activation of solid state displacement reactions with ball milling. Thus, mechanical energy is used to induce chemical reactions. The chemical precursors typically consist of mixtures of oxides, chlorides and/or metals that react either during milling or during subsequent heat treatment to form a composite powder consisting of the dispersion of ultrafine particles within a soluble salt matrix. The ultrafine particle is then recovered by selective removal of the matrix phase through washing with an appropriate solvent. Mechanochemical synthesis is generally based on the following displacement reaction:

$$AxC + yB \rightarrow xA + ByC$$

In the equitation, AxC and B are precursors, A is the desired product and ByC is a by-product of the reaction. This process has been used successfully to prepare nanoparticles

of a number of materials, including transition metals, oxide ceramics, and oxide semiconductors.

1.3 Magnetic metal oxide nanoparticles and their applications [43-49]

Magnetic nanoparticles are of special interest owing to their unique magnetic properties due to their reduced size (< 100 nm). Magnetic nanoparticles have potential use in many technological applications. Depending on the type of applications, magnetic nanoparticles are used in varieties of forms such as surface functionalized particles in biomedical applications, as particle arrays in magnetic storage media, as compacted powders in permanent magnets and in solutions as ferrofluids.

Magnetic nanoparticles have been proposed for biomedical applications for several years. Recently, nanotechnology has developed to a stage that makes it possible to produce, characterize and specifically tailor the functional properties of nanoparticles for applications. This shows considerable promise for applications in biomedical and diagnostic fields such as targeted drug delivery, hyperthermia treatment for malignant cell, and magnetic resonance imaging (MRI). There are three reasons why the magnetic nanoparticles are useful in biomedical applications. First, magnetic nanoparticles can have controllable size ranging from a few nanometers up to tens of nanometers, and are smaller than comparable in sizes to a cell (10-100μm), a virus (20-450 nm), a protein (5

-50 nm) or a gene DNA segment (2nm wide and 10 -100 nm long). They can get close to the cell or gene and they can be coated with bio-molecules to make them interact or bind with a biological entity. Second, magnetic nanoparticles can be manipulated by an external magnetic field gradient. They can be used to deliver a package, such as an anticancer drug to a targeted region of the body such as a tumor. Third, magnetic nanoparticles can also be made to resonantly respond to a time-varying magnetic field, with an associated transfer of energy from the field to the nanoparticles. They can be made to heat up, which leads to their use as hyperthermia agents, delivering toxic amounts of thermal energy to targeted bodies such as tumors. As highlighted above for biomedical application, magnetic nanoparticles must (i) have a good thermal stability; (ii) have a larger magnetic moment; (iii) be biocompatible; (iv) be able to form a stable dispersion so the particles could be transported in living systems; (v) respond well to AC magnetic fields. Furthermore, better control of particle size and properties will be necessary to use these particles in biomedical applications, in which uniformity of the properties will ensure accurate dosing and delivery. The most widely used magnetic nanoparticles for biomedical applications are magnetite (Fe_3O_4) and related oxides which are chemically stable, nontoxic, non-carcinogenic and have attractive magnetic properties.

Magnetic oxide nanoparticles can also be used for magnetic recording media which require a small material grain, narrow size distribution, thermal stability and very high magnetic anisotropy energy Ku. $CoFe_2O_4$ nanoparticles are well-known material with very high cubic magnetocrystalline anisotropy, good coercivity, and moderate saturation magnetization. These properties make $CoFe_2O_4$ nanoparticles a promising

material for high-density magnetic recording devices. Furthermore, the magnetic metal oxide nanoparticle can also be used for magnetic separation and ferrofluid applications.

1.4 Semiconductor nanocrystals and their applications [50-52]

During the past decade, tremendous advances in colloid chemistry have led to the preparation of high quality nanometer sized semiconductor crystals. Semiconductor QDs are inorganic nanoparticles that contain hundreds to several thousands of atoms. When the size of semiconductor nanocrystals is smaller than the Bohr radius of the excited electron-hole pair, quantum confinement effect occurs and the band gap energy starts to increase with the decrease of particle size. The unique electronic, optical, and catalytic properties of semiconductor nanoparticles, with the different methods available for the preparation of nanoparticles of controlled shape and size, provide exciting building blocks for nanoscale assembies, structures, and devices.

A variety of synthetic methodologies for the preparation of nanoparticles within a narrow size distribution are available. Often, the nanoaprticles are prepared by "wet chemistry" procedures, in which clusters of semiconductor molecules are formed in the presence of a surface-capping ligand. This capping igand binds to the semiconductor cluster, prevents aggregation of the particles into bulk material, and control the final dimensions of the nanoparticles. Many capping systems are available: hydrophobic monolayers, positively or negatively charged hydrophilic monolayers, and polymer layers. Association of molecular units to the nanoparticles introduces chemical functionalities that can provide recognition or affinity interactions between different appropriately

modified particles and thereby dictate the structure when aggregation occurs. New collective properties of aggregated nanoparticles, such as coupled-plasmon absorbance, interparticle energy transfer, and electron transfer or conductivity, may be observed in the cluster assemblies.

Currently, one of the main research interests in the field of semiconductor nanoclusters is their optical properties. It is expected that these semiconductor nanocluster or quantum dots will greatly contribute to the fields of biology and biochemistry by taking advantage of their attractive luminescence properties: broad excitation-narrow emission photophysics, size-tunable emission, longer fluorescence lifetime, and negligible photobleaching. All these unique properties make semiconductor nanoparticle a good candidate for bio-application. For example, monitoring living cells in vivo can be realized by tracking the luminescence from the nanaparticles bioconjugated to target species.

1.5 Silica particles formation in homogeneous solution and microemulsions [53-57]

1.5.1 Stober method

In 1956, Gerhard Kolbe published the first results that showed that spherical silica particles could be precipitated from tetraethoxysilane in alcohol solution when ammonia was present as the catalyzing base. Several years later, in 1968, Stober continued in this

research area and published the frequently cited article for the preparation of monodispersed silica particles from alkoxide solutions. Stober and his colleagues improved the precipitation process and described the formation of exceptionally monodispersed silica particles. The final size could be controlled over a wide range from about 50 nm to 1 ½ um. Variations of the particle size could be achieved by different means, for example, temperature, water and ammonia concentration, type of alcohol (solvent), TEOS (tetraethoxysilane) concentration, or mixing conditions.

The process did not draw too much attention until about 20 years later when several research groups started to apply those monodispersed silica particulates in various studies and the particle formation and growth process was studied in more detail. Numerous applications have been demonstrated for the "Stober" silica particles such as chemically modified silica surface, chromatography, dyes and pigments, ordered packing and controlled pore structure, and sintering studies. The main advantages of the Stober silica particles are that the particles are exceedingly uniform in size, the size can be easily controlled, and the overall process proceeds at relative high concentrations and thus yields larger amounts of powders at comparable low cost. Several companies have adopted the production process, for example, the materials are used in special chromatography applications.

The original process was described by Stober, Fink and Bohn. A suitable alkoxysilane is reacted in the corresponding alcohol, water, and ammonia mixture. Usually the reaction is performed at room temperature, but higher or lower temperatures

can also be applied, if so desired. Stober and his coworkers described the influence of different alkoxides and alcohols as well as the water and ammonia concentration on the resulting particle size. With slight variations, the Stober silica precipitation process proceeds from the same chemicals. The starting material is TEOS, tetraethoxysilane, $Si(OC_2H_5)_4$; the solvent is an alcohol (preferably ethanol); water is added; and ammonia acts as the catalyst to initiate the hydrolysis and condensation reaction. In a very brief schematic way the reaction could be described as follows:

Hydrolysis:

$$Si(OC_2H_5)_4 \xrightarrow{+H_2O - HOC_2H_5} Si(OC_2H_5)_3OH$$

$$\xrightarrow{+H_2O - HOC_2H_5} Si(OC_2H_5)_2(OH)_2 \text{ etc.}$$

Condensation:

$$Si(OC_2H_5)_3OH \xrightarrow{+Si(OC_2H_5)_3OH - H_2O} (H_5C_2O)_3Si\text{-}O\text{-}Si(OC_2H_5)_3 \text{ etc.}$$

$$\longrightarrow SiO_2 \text{ particle}$$

The formation of silica particles is only in part influenced by the purity of the chemical constituents. However, pure chemicals and here especially the purity of the TEOS will help to get reproducible results as well as to achieve narrow particle size distributions.

1.5.2 Silica formation by microemulsion method

Silica synthesis via the microemulsion-mediated alkoxide sol-gel process is another important and useful approach. This technique generally available for the solution synthesis of nanoparticles may be broadly classified into those that rely on microreactors, and those that exploit growth modifiers. In microreactor techniques, crystal growth is constrained by forcing particle formation to occur in small isolated volumes. On the other hand, in the case of techniques that rely on growth modifiers, chemical additives such as organic solvent, organic polymers, etc. are introduced into the reaction medium to modify the rate of particle nucleation, growth, or aggregation. Microemulsions, as reaction media, are unique in that they offer both microreactor and growth-modifier capabilities. In the water-in-oil (w/o) variety of these compartmentalized fluids, fine microdrops of aqueous phase (2-30 nm) are trapped within aggregates of surface-active molecules dispersed in an external oil phase. The dispersed water pools constitute spatially separated nanoreactors that allow the solubilized reacting species to be distributed at the molecular level. At the same time, the surfactant-stabilized microcavities (reverse micelles) provide a cage-like effect that limits particle nucleation, growth, and aggregation.

Alkoxide-based silica are typically derived from tetramethoxysilane [$Si(OCH_3)_4$, TMOS] and tetraethoxysilane [$Si(OCH_2CH_3)_4$, TEOS] as precursors. The silica formation process can be conveniently viewed in terms of a hydrolysis step, that generates silanol group (-SiOH), followed by polycondensation reactions, that form silicon-oxygen-silicon bonds.

$$Si(OR)_4 + {}_XH_2O \rightarrow Si(OR)_{4-x}(OH)_X + {}_XROH$$

$$Si\text{-}OH + HO\text{-}SI \rightarrow Si\text{-}O\text{-}Si + H_2O$$

$$Si\text{-}OH + RO\text{-}Si \rightarrow Si\text{-}O\text{-}Si + ROH$$

These reactions are responsive to both acid and base catalysis, and can be manipulated to give a variety of silica products, such as discrete particles, monolithic gels, films, and fibers. This technique of materials synthesis via alkoxide hydrolysis has become known as sol-gel processing. The first attempt to extend the alkoxide sol-gel process to microemulsion systems was reported by Yanagi in 1986. Since then, more than hundreds of additional contributors have devoted their research on this topic. In the microemulsion-mediated sol-gel process, the microheterogeneous nature (the polar-nonpolar character) of the microemulsion fluid phase permits the simultaneous solubilization of the relatively hydrophobic alkoxide precursors and the reactant water molecules. The alkoxide molecules encounter water molecules in the polar domains of the microemulsions, the resulting hydrolysis and condensation reactions can lead to the formation of nanosize silica particles.

1.6 Coated particles

For many reasons, it may be advantageous to cover one kind of particles with a layer of a different chemical composition. In doing so it is possible to alter optical,

magnetic, electric, catalytic, adsorptive, and other properties of the original dispersion. Furthermore, one may produce particles of a given morphology, if the latter cannot be achieved directly, by selecting the core of the desired shape and encasing it with a shell of the material of interest.

In principle, the coating may be produced in two ways, i.e., by (1) interacting the cores with preformed smaller particles of a different composition (essentially by heterocoagulation), and (2) by forming a shell directly by chemical reaction on the preformed particles dispersed in salt solutions yielding the coating. In both instanced it is essential that conditions be optimized in order to avoid having mixed dispersions of coated and constituent particles.

Coated particles can enhance the unique properties of the core particles and extend the application to various areas. For example, the shell of ZnS has been used to coat the luminescence CdS or CdSe quantum dots, which prevent the surface passivation and enhance the optical property of the core quantum dots. In the case of the magnetic ferrite nanoparticles, we would like the particles to be stable, water soluble and compatible to some bio-molecules for different applications. So coating another layer of materials on the surface of magnetic particles is essential for those requirements. Silica is one of the most important coating materials because it is stable, transparent and most of all, silica is easily manipulated to be compatible with bio-applications.

In the later chapter, we will discuss the silica shell coating on the magnetic and semiconductor nanoparticles. Also we would like to discuss the polymer coating via a direct chemical reaction.

1.7 Reference

1. Ratner, M; Ratner, D, *Nanotechnology: A Gentle Introduction to the Next Big Idea*, Person Education, Inc., **2003**.
2. A. Eychmuller, *J. Phys. Chem. B,* **2000**, *104*, 6514.
3. N. R. Rao, A. Mueller, A. K. Cheetham, *The Chemistry of Nanomaterials: Synthesis, Properties and Applications, Vol.1*, Wiley-VCH, Weinheim, **2004**.
4. C. J. Brinker, G. W. Scherer, *Sol-Gel Science*. *Academic Press* **1990**.
5. C. Sanchez, J. Livage, *New J. Chem.* **1990**, *14*, 513.
6. C. J. Brinker, Y. F. Lu, A. Sellinger, H. Y. Fan, *Adv. Mater.* **1999**, *11*, 579.
7. G. M. Whitesides, B. Grzybowski, *Science* **2002**, *295*, 2418.
8. P. D. Yang, D. Y. Zhao, D. I. Margolese, B. F. Chmelka, G. D. Stucky, *Nature* **1998**, *396*, 152.
9. D. M. Antonelli, J. Y. Ying, *Chem. Mater.* **1996**, *8*, 874.
10. A. Corma, P. Atienzar, H. Garcia, J. Y. Chane-Ching, *Nat. Mater.* **2004**, *3*, 394.
11. S. Deshpande, N. Pinna, B. Smarsly, M. Antonietti, M. Niederberger, *Small* **2005**, *1*, 313.

12. J. Ba, J. Polleux, M. Antonietti, M. Niederberger, *Adv. Mater.* **2005**, *17*, 2509.

13. G. J. d. A. A. Soler-Illia, C. Sanchez, B. Lebeau, J. Patarin, *Chem. Rev.* **2002**, *102*, 4093.

14. G. Göltner, M. Antonietti, *Adv. Mater.* **1997,** *9,* 431.

15. S. Förster, M. Antonietti, *Adv. Mater.* ***19*98,** *10,* 195.

16. G. A. Ozin, *Chem. Comm.* **2000,** 419.

17. Grosso, G. J. d. A. Soler-Illia, E. L. Crepaldi, F. Cagnol, C. Sinturel, A. Bourgeois, A. Brunet-Bruneau, H. Amenitsch, P. A. Albouy, C. Sanchez, *Chem. Mater.* **2003,** *15,* 4562.

18. Grosso, F. Cagnol, G. J. de A. A. Soler-Illia, E. L. Crepaldi, H. Amenitsch, A. Brunet-Bruneau, A. Bourgeois, C. Sanchez, *Adv. Funct. Mater.* **2004,** *14,* **3**09.

19. Grosso, C. Boissiere, B. Smarsly, T. Brezesinski, N. Pinna, P. A. Albouy, H. Amenitsch, M. Antonietti, C. Sanchez, *Nat. Mater.* **2004,** *3,* 787.

20. R. A. Caruso, M. Antonietti, *Chem. Mater.* **2001,** *13,* **32**72.

21. R. A. Caruso, *Top. Curr. Chem.* **2003**, 226**,** 91.

22. B. Chu, B. S. Hsiao, *Chem. Rev.* **2001**, *101*, 1727.

23. A. R. West, *Basic Solid State Chemistry-Second Edition*, John Wiley & Sons, Ltd., **1995**.

24. IUPAC, *Pure and Applied Chemistry* **1972**, *31*, 578.

25. S. J. Gregg, K. S. W. Sing, *Adsorption, Surface Area and Porosity-2nd Edition*, Academic Press Limited. United Kingdom. **1997**.

26. M. Kruk, M. Jaroniec, *Chem. Mater.* **2001**, *13*, 3169

27. C. Burda, X. Chen, R. Narayanan, M. A. El-Sayed, *Chem. Rev.* **2005**, *105*, 1025.

28. A.P. Alivisatos, *J. Phys. Chem.* **1996**, *100*, 13226.

29. Henglein, *Chem. Rev.* **1989**, *89*, 1861.

30. M. L. Steigerwald, L. E. Brus, *Acc. Chem. Res.* **1990**, *23*, 183.

31. M. A. El-Sayed, *Acc. of Chem. Res.* **2004**, *37*, 326.

32. R. Rossetti, S. Nakahara, L. E. Brus, *J. Chem. Phys.* **1983**, *79*, 1086.

33. Burda, X. Chen, R. Narayanan, M. A. El-Sayed, *Chem. Rev.* **2005**, *105*, 1025.

34. A. P. Alivisatos, *J. Phys. Chem.* **1996**, *100*, 13226.

35. A. Henglein, *Chem. Rev*. **1989**, *89*, 1861.

36. M. L. Steigerwald, L. E. Brus, *Acc. Chem. Res*. **1990**, *23*, 183.

37. M. A. El-Sayed, Acc. of Chem. Res. **2004**, 37, 326.

38. R. Rossetti, S. Nakahara, L. E. Brus, *J. Chem. Phys*. **1983**, *79*, 1086.

39. R. Rossetti, J. L. Ellison, J. M. Gibson, L. E. Brus, *J. Chem. Phys*. **1984**, *80*, 4464.

40. L. Cushing, V. L. Kolesnichenko, C. J. O'Connor, *Chem. Rev*. **2004**, *104*, 3893.

41. M. Jansen, Angew. *Chem. Int. Ed.* **2002**, *41*, 3747.

42. J. Gopalakrishnan, *Chem. Mater*. **1995**, *7*, 1265.

43. L. G. Hubert-Pfalzgraf, *J. Mater. Chem*. **2004**, *14*, 3113.

44. J. Livage, M. Henry, C. Sanchez, *Prog. Solid St. Chem*. **1988**, *18*, 259.

45. C. Matijevic, *Chem. Mater*. **1993**, *5*, 412.

46. A. W. Dearing, E. E. Reid, *J. Am. Chem. Soc*. **1928**, *50*, 3058.

47. B. Vioux, *Chem. Mater*. **1997**, *9*, 2292.

48. J. N. Hay, H. M. Raval, *Chem. Mater*. **2001**, *13*, 3396.

49. T. Hyeon, *Chem. Commun*. **2003**, 927.

50. Y. W. Jun, J. H. Lee, J. S. Choi, J. Cheon*, J. Phys. Chem. B* **2005***, 109*, 14795.

51. M. Niederberger, M. H. Bartl, G. D. Stucky, *Chem. Mater*. **2002**, *14*, 4364.

52. N. Pinna, M. Antonietti, M. Niederberger, *Colloids Surf., A* **2004**, *250*, 211.

53. N. Pinna, G. Neri, M. Antonietti, M. Niederberger, Angew. *Chem. Int. Ed*. **2004**, *43*, 4345

54. N. Pinna, G. Garnweitner, M. Antonietti, M. Niederberger, Adv. Mater. **2004***, 16*, 2196.

55. M. Niederberger, N. Pinna, J. Polleux, M. Antonietti, Angew. *Chem. Int. Ed*. **2004**, *43*, 2270.

56. M. Niederberger, G. Garnweitner, F. Krumeich, R. Nesper, H. Cölfen, M. Antonietti, *Chem. Mater*. **2004,** *16*, 1202.

57. J. Ba, J. Polleux, M. Antonietti, M. Niederberger, *Adv. Mater*. **2005,** *17*, 2509.

Chapter 2 EXPERIMENTAL SECTION

2.1. SYNTHESIS TECHNIQUES

2.1.1 High temperature solution phase synthesis [1-14]

A general scheme for preparing monodisperse NC samples requires a single, temporally short nucleation event followed by slower growth on the existing nuclei. This may be achieved by rapid addition of reagents into a reaction vessel containing a hot, coordinating solvent. The temperature of the solution is sufficient to decompose the reagents, forming a supersaturation of species in solution that is relieved by nucleation of NCs. Upon nucleation the concentration of these species in solution drops below the critical concentration for nucleation, and further material can only add to the existing nuclei.

An alternative synthetic approach involves mixing the reagents in a vessel at a temperature low enough to preclude any appreciable reaction. A controlled ramp of the solution temperature accelerates the chemical reaction and produces the requisite super saturation, which is then relieved by a burst of nucleation. As long as the temperature is adjusted to keep the rate at which the reagents react less than or equal to the rate at which material adds to the existing nuclei, the supersaturated state is never revisited and no new nuclei form. In either approach, the size distribution of the NC sample is limited primarily by the short time interval in which the nuclei form and begin to grow.

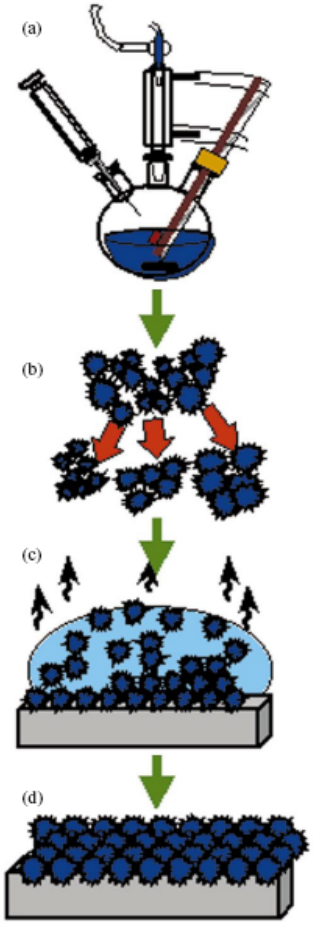

The systematic adjustment of the reaction conditions— time, temperature, and concentration and chemistry of reagents and surfactants— can be used to control NC size and thus prepare a size series of NC samples. In general, NC size increases with increasing reaction time, as more material adds to NC surfaces, and with increasing temperature, as the rate of addition of material to the existing nuclei increases.

2.1.2 Microemulsion method[15-19]

Hoar and Schulman noted in 1943 that certain combinations of water, oil, surfactant and alcohol or amine-based co-surfactant produced clear, seemingly homogeneous

solutions that he later termed "micro emulsions." The oil phases, in this case, were simple long-chain hydrocarbons and the surfactants were long-chain organic molecules with a hydrophilic head (usually an ionic sulfate or quarternary amine) and lipophilic tail. The amphiphilic nature of the surfactants makes them miscible in both hydrocarbons and water, but when the surfactant is mixed with a hydrocarbon, the resulting mixture, although optically isotropic, cannot be properly described as a solution. The surfactant, through ion-dipole interactions with the co-surfactant, will form spherical aggregates in which the polar ends of the surfactant molecules orient towards the center. Likewise, the addition of water to the system will cause the aggregates to expand from center as the water molecules (again as a result of ion-dipole and dipole-dipole interactions) situate at the center of the sphere.

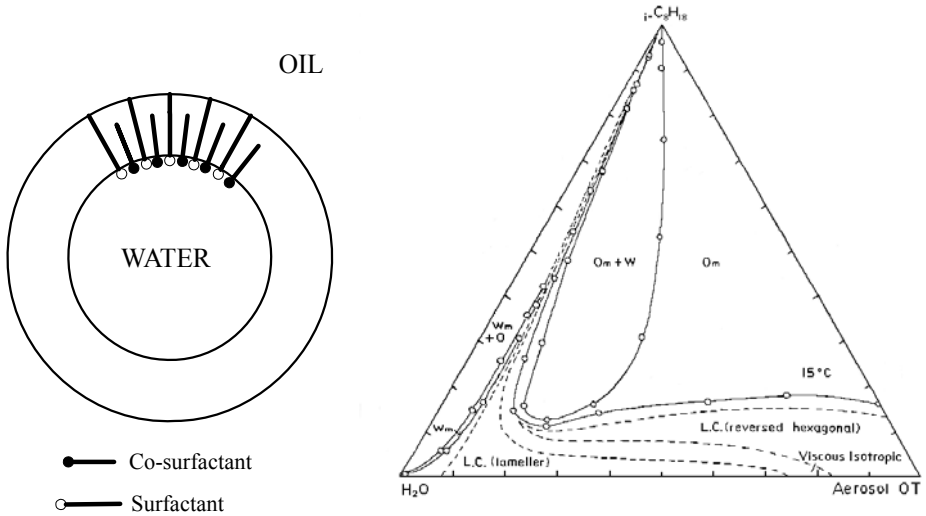

Figure **1A.** The formation of a representative surfactant-oil-water system

Figure **1B.** A schematic phase diagram of water-in-oil droplet

The spherical aggregates described represented in Figure 1A are commonly referred to as reverse micelles, and are generally characterized by *o*, the molar ratio of water to surfactant: $o = [H_2O] / [Surfactant]$. By controlling the ratio of water to surfactant, we can adjust the size of the water droplet. Thus, this method provides a good mechanism to control the size of the nanoparticles formed in the aqueous cores. Figure 1B is the schematic phase diagram of a sample surfactant-oil-water system. Based on the diagram, we can find the critical condition to form stable reverse micelles, which exist only over a narrow composition range.

2.2. ANALYSIS AND CHARACTERIZATION

2.2.1 X-ray Powder Diffraction[20]

The X-ray powder diffraction (XRD) diagrams of all samples (except iron) were collected on a Phillips-X'PERT Diffractometer (Cu, Ka= 1.54056 Å) source with a graphite monochrometer. The data collection and analysis were carried out using the software supplied with the diffractometer. Particle's size can be calculated by the Scherrer equation: $Dc=K\lambda/\beta\cos\theta$. Where Dc accounts for the average crystal size (here the diameter of the nanoparticles), K = 0.89 is the Scherrer coefficient, λ denoting the X-ray wavelength is equal to Ka (shown above). β is the full width at half-maximum (FWHM) and θ is the diffraction angle.

2.2.2 Transmission Electron Microscopy (TEM)[21]

Transmission electronic microscopy (TEM) is widely used to observe the morphology of the nanoproducts and to check their uniformity. By using TEM, a large variety of materials such as ceramics, minerals, metals, alloys, semiconductors, glass and polymers can be observed. The main requirements for the samples are: they must not outgas due to the high vacuum ambient of work, and they have to be appropriately thinned to be observed. In our work, TEM investigations were performed on a JEOL 2010 microscope. For the investigation of the longitudinal shape and structure, the nano-material was deposited onto a perforated carbon foil supported on a copper grid.

2.2.3 Energy Dispersive Spectroscopy (EDS)

Elemental analysis was carried out using an EDAX attachment on a JEOL 2010 TEM with the electron beam focused to two nanometers. EDS is a method of X-ray analysis, which discriminates by energy levels the characteristic X-rays emitted from a sample. The EDS system uses a solid-state detector, which receives counts of all X-rays at once, and divides the energy spectrum of X-rays into different ranges. A collection of X-ray energies from 0 to 40 KeV, can be collected and displayed on a computer screen. Peaks will show up on the spectrum, corresponding to energies of elements present in the sample. The area included within a peak is roughly proportional to the amount of the corresponding element in the sample, although the detector efficiency decreases with increasing energy. The EDS system can be used for quantitative analysis by counting the

X-rays received in the channels that correspond with a peak of interest. EDS is a quick way to find out what is in a sample.

2.2.4 Fourier Transform Infrared (FT-IR)[22]

A FT-IR spectrometer (Thermo Nicolet NEXUS 670 FT-IR) was employed to characterize the surface properties of the nanoproducts, especially for polymer coated nanocomposites. FT-IR is most useful for identifying chemicals that are either organic or inorganic. It can be utilized to quantitate some components of an unknown mixture. It can be applied to the analysis of solids, liquids, and gasses.

The term Fourier Transform Infrared Spectroscopy (FT-IR) refers to a fairly recent development in the manner in which the data is collected and converted from an interference pattern to a spectrum. Today's FT-IR instruments are computerized which makes them faster and more sensitive than the older dispersive instruments.

2.2.5 UV-visible spectroscopy[23]

UV-vis spectroscopy probes the electronic transitions of molecules as they absorb light in the UV and visible regions of the electromagnetic spectrum. Any species with an extended system of alternating double and single bonds will absorb UV light, and anything with color absorbs visible light, making UV-vis spectroscopy applicable to a wide range of samples. Since gold has Plasmon property, UV-Visible was employed to measure some gold related information.

2.2.6 Inductively Coupled Plasma (ICP)[24]

ICP analysis was performed with CCD Simultaneous ICP- optical emission spectrometry (OES) spectrometer to analyze the composition in the nanoproducts. In the ICP-OES, plasma is used as an energy source, producing heat of 5500° - 8000°K and up to 10000°K in some regions, enough to ionize and excite most analytic atoms. Upon the electron's decay to its ground state, light is emitted and detected. Because the excited ion only emits light of certain wavelengths, spectral lines dependent on the element are produced. These lines can then be used to qualitatively determine the components of the sample. A calibration curve of spectra intensity and concentration can be used to quantitatively determine the concentration of analytic in the sample.

2.2.7 ThermoGravimetric Analysis (TGA)[25]

Thermal Analyst 2000 Thermogravimetric Analyzer was employed. Thermogravimetry is one of the oldest thermal analytical procedures and has been used extensively in the study of polymeric systems. The technique involves monitoring the weight loss of the sample in a chosen atmosphere (usually nitrogen or air) as a function of temperature. The usefulness of TGA for analyzing complex systems such as rubber vulcanites was greatly enhanced by the introduction of the ability to record simultaneously the first derivative of the weight loss. This is sometimes referred to as derivative thermogravimetric analysis (DTG). The method can not only give us the

composition ratio in the nanoproducts, but also give us the information of the composition.

2.2.8 Magnetic measurement[26]

Magnetic measurements were performed on a SQUID magnetometer (MPMS 5S, Quantum Design). A SQUID detector is a state-of-the-art superconducting susceptometer with a Josephson junction element. It is capable of amplifying very small changes in a magnetic field into a large electrical signal. It can therefore measure a magnetic susceptibility as small as 10^{-10} emu over a wide temperature range (near 0 K to 400 K).

The magnetic measurements include magnetic susceptibility and magnetization. Magnetic susceptibility can be measured as a function of temperature in the presence of a static magnetic field (*DC-M/H*), an alternating magnetic field (*AC-dM/dH*) or both. Typically, samples were characterized utilizing *DC* susceptibility and magnetization as a function of field measurements. A *DC* measurement can be done with two different methods. Either the sample is cooled in the presence of a magnetic field or in the absence; e. g., *FC* (field cooling) and *ZFC* (zero field cooling). In a field cooled experiment the sample is loaded at room temperature and cooled in the presence of a magnetic field. This causes the spins of the sample to align with the external field. In a zero field cooled experiment the sample is loaded at room temperature and cooled in the absence of a field. This allows the spins to align randomly. In typical bulk samples the external measuring field is not sufficient to overcome the natural ordering of the samples, therefore, the *FC*

and *ZFC* susceptibility curves look similar. In spin glass and superparamagnetic materials, however, there is marked difference in the two curves. Field cooled (*FC*) and zero field cooled (*ZFC*) magnetization experiments at low field are very useful for elucidating superparamagnetic properties. They are simple and point out the irreversible properties below a certain temperature, roughly the mean blocking temperature TB related to the characteristic time of the experiment.

However, quantitative features can be obtained only with a precise analysis of the phenomenon. This detailed analysis depends on the experimental process and on the sample parameters, such as, the volume distributions, the particle arrangement, the interaction effects, and so on. Much information can be derived from such an analysis concerning mainly the barrier energy distribution and the related volume distributions. The particle magnetic state, the effect of the interparticle interactions from dynamic as well as static points of view can be derived.

2.3 Reference

1. E. C. Stoner and E. P. Wohlfarth, *Phil. Trans. Roy. Soc. A.* **1948**, *240***,** 599 – 642
2. F. E. Luborsky, *J. Appl. Phys.* **1961**, *32***,** 171–183.
3. A. Aharoni, *Introduction to the Theory of Ferromagnetism*, *Oxford University Press, New York*, **1996**, pp. 133–152.
4. S. Morup, A. Hernando, Ed., *Kluwer Academic Publishers*, Boston, **1993**, pp. 93–99.

5. S. Sun, C. B. Murray, D. Weller, L. Folks, and A. Moser, *Science.* **2000**, *287***,** 1989 –1992.
6. S. V. Gaponenko, *Cambridge University Press, Cambridge, England*, **1998**.
7. U. Woggon, *Springer-Verlag, Berlin*, **1997**.
8. A. P. Alivisatos, *Science.* **1996**, *271***,** 933–937.
9. C. B. Murray, C. R. Kagan, and M. G. Bawendi, *Ann. Rev. Mater. Sci.* **2000**, *30*, 545– 610.
10. S. Sun, C. B. Murray, and H. Doyle. *Mater. Res. Soc. Symp. Proc.* **1999**, *577***,** 385–398.
11. C. B. Murray, D. J. Norris, and M. G. Bawendi, *J. Am. Chem. Soc.* **1993**, *115*, 8706 – 8715.
12. C. B. Murray, C. R. Kagan, and M. G. Bawendi, *Science* **1995**, *270***,** 1335–1338.
13. C. R. Kagan, C. B. Murray, and M. G. Bawendi, *Phys. Rev. B* **1996**, *54***,** 8633–8643.
14. C. B. Murray, Shouheng Sun, W. Gaschler, H. Doyle, T. A. Betley, C. R. Kagan., *IBM J. RES. & DEV.* **2001,** *45,* 1
15. Hoar, T. P.; Schulman, J. H. *Nature* **1943**, *152*, 102.
16. Pileni, M.P., *Langmuir,* **1997**, 13, 3266
17. Song-Yuan Chang, Lei Liu, Sanford A. Asher,. *J. Am. Chem. Soc*.; **1994**; *116*; 6739-6744
18. Martino, A.; Yamanaka, S. A.; Kawola, J. S.; Loy, D. A., , *Chem. Mater*.; **1997**, *9*, 423-429.

19. Jain, T. K.; Roy, I.; De, T. K.; Maitra, A., , *J. Am. Chem. Soc*, **1998**; *120*, 11092-11095.

20. Jenkins, R.; Snyder, R. L. *Introduction to X-ray powder Diffractometry*, **1996**, *John Wiley &Sons, Inc*..

21. Williams, D. B.; Carter, C. B. *Transmission Electron Microscopy: A Textbook for Materials Science*, **1996**, *Plenum US*.

22. Ferraro, J. R.; Basile, L. J. *Fourier Transform Infrared Spectroscopy: Applications to Chemical Systems (vol. 1)*, **1978**, *Academic Press*.

23. Misra, P.; Dubinskii, M. A. *Ultraviolet Spectroscopy and UV Lasers,* **2002**, *Marcel Dekker*.

24. Nolte, J. *ICP Emission Spectrometry: A Practical Guide,* **2003**, *Wiley-VCH*.

25. Keattch, C. J. *An Introduction to Thermogravimetry*, **1969**, Heyden, in co-operation with Sadtler Research Laboratories, Philadelphia.

26. O'Connor, C. J.; Tang, J.; Zhang, J. H. *Nanosize Magnetic Particles, MagnetoScience: Molecules to Materials,* ed. by J. S. Miller and M. Drillon, **2001**, *Wiley-VCH, New York*.

CHAPTER 3 SYNTHESIS OF METAL OXIDE NANOPARTICLES IN NONAQUEOUS SOLVENT

3.1 Introduction

Nano-scale metal oxide particles of uniform size are intensively drawing attention because they exhibit significantly enhanced chemical, thermal, optical, electrical, magnetic, and catalytic properties. Because physical and chemical properties of nanomaterials depend not only on the composition but also on particle size and shape, the proper synthesis protocol first of all has to provide control over particle size and shape. Further requirements are control over surface properties and particle size distribution, because both parameters are important with respect to the use of nanoparticles as building blocks for assembly into larger nanostructures, high crystallinity and purity (phase purity in terms of polymorph mixtures and low amount of other impurities), good yields and general applicability of the synthesis methodology. Lots of researchers devote their effects on the area of metal oxides synthesis and try to get the optimum conditions to control the particle morphology as well as chemical composition. Among the various synthesis approaches reported in the last few years, wet chemistry synthetic route such as high temperature nonaqueous solution route is particularly promising to fulfill most of these requirements and it allows good control over the particle size, shape, surface structure and size distribution. Comparing with some other physical methods which used to produce larger amount of metal oxide particle, the wet chemistry method would

provide more reaction parameters which can be varied in order to achieve a better control over the morphology of the resulting nanocrystals.[1-14]

3.2 Synthesis of metal oxide nanoparticles in nonaqueous organic solvent at high temperature and their characterization

3.2.1 Introduction

Although nanochemistry is a particularly fast developing research area, nanoparticle synthesis is still a major part of it. The reason lies in the fact that nanomaterials have to exhibit many specific features in order to meet all the expectations that are related to their tiny size.

Before we discuss the nonaqueous solvent reaction, we should get to know the basic principles and limitation of aqueous sol-gel chemistry. It is not surprising that the concepts of aqueous sol-gel chemistry, which had a long and successful tradition in the synthesis of bulk metal oxides, have been adapted for nanoparticle synthesis. However, aqueous sol-gel chemistry suffers from some major drawbacks, which affect nanoparticle synthesis much more than in the case of bulk metal oxides. In the most cases the as-synthesized precipitates are amorphous and subsequent heat treatment is necessary to induce crystallization.

This additional step results either in alteration, mainly particle growth, or even destruction of the well-defined particle morphology. Further disadvantages of aqueous

systems are reaction parameters that are difficult to control, such as fast hydrolysis rate, PH, method of mixing, rate of oxidation and especially the nature and concentration of anions. Nonaqueous (or non-hydrolytic) processes in organic solvents are able to overcome many of the specific problems typical for aqueous systems.

Nonaqueous solution routes to metal oxide nanoparticles are a valuable alternative to well-known aqueous sol-gel processes, offering advantages such as high crystallinity at low temperatures, robust synthesis parameters and ability to control the crystal growth without the use of surfactants. We will discuss the various nonaqueous routes to metal oxides, their surface functionalization and their assembly into well defined nanostructures. However, we will strongly focus on the synthetic processes developed in our group. Within the various reaction systems such as metal halides—diethylene glycol (DEG), metal acetylacetonates—benzyl ether/phenyl ether, metal acetates — long chain hydrocarbon and metal acetates —oleic alcohol we will discuss representative several kinds of technologically interesting crystalline metal oxide such as magnetite and indium oxide as examples in order to show the versatility of this approach. Furthermore, we will discuss how the reaction parameters such as the ratio of capping ligands and temperature affect the particles size and shape.[15-21]

3.2.2 Magnetite NPs (Fe_3O_4)

Magnetic nanoparticles have applications in information storage, color imaging, magnetic refrigeration, bioprocessing, medical diagnosis, controlled drug delivery, and as ferrofluids. Thus, developing a new synthetic route for magnetic nanoparticles and

investigating their properties are of immense importance. Ferrites, the transition metal oxides having a spinel structure, are technologically important because of their appealing magnetic and electrical properties. The uniform particle size and distribution are essential to satisfy those applications. [22-27]

The general synthesis approach is list as following: Iron (III) acetylacetonate, 1,2-hexadecanediol, oleic acid, oleylamine and benzyl ether were mixed and magnetically stirred under argon atmosphere. The mixture was heated to 200 °C for 2 h and then heated to reflux (~300 °C) for 1 h. The black-colored mixture was cooled to room temperature and collected by centrifugation after diluting the sample with sufficient amount of ethanol. The oleic acid stabilized magnetic particles were re-dispersed in hexane and used as precursors for seed-mediated growth. [28-37]

3.2.2.1 Synthesis of 4 nm Fe_3O_4 Nanoparticle Seeds.

$Fe(acac)_3$ (2 mmol), 1,2-hexadecanediol (10 mmol), oleic acid (6 mmol), oleylamine (6 mmol), and phenyl ether (20 mL) were mixed and magnetically stirred under a flow of nitrogen. The mixture was heated to 200 °C for 30 min and then, under a blanket of nitrogen, heated to reflux (265 °C) for another 30 min. The black-brown mixture was cooled to room temperature by removing the heat source. Under ambient conditions, ethanol (40 mL) was added to the mixture, and a black material was precipitated and separated via centrifugation. The black product was dissolved in hexane with the small extra amount of oleic acid (0.05 mL) and oleylamine (0.05 mL). Centrifugation (4000

rpm, 15 min) was applied to remove any un-dispersed residue. The product, 4 nm Fe_3O_4 nanoparticles, was then precipitated with sufficient ethanol, centrifuged again (4000 rpm, 15 min) to remove the solvent, and re-dispersed into hexane.

3.2.2.2 Synthesis of 6 nm Fe_3O_4 Nanoparticle Seeds.

$Fe(acac)_3$ (2 mmol), 1,2-hexadecanediol (10 mmol), oleic acid (6 mmol), oleylamine (6 mmol), and benzyl ether (20 mL) were mixed and magnetically stirred under a flow of nitrogen. The mixture was heated to 200 °C for 2 h and then, under a blanket of nitrogen, heated to reflux (~300 °C) for 1 h. The black-colored mixture was cooled to room temperature by removing the heat source. Following the workup procedures described in the synthesis of 4 nm particles, a black-brown hexane dispersion of 6 nm Fe_3O_4 nanoparticles was produced.

3.2.2.3 Synthesis of larger Fe_3O_4 Nanoparticles by seed mediated growth

The larger magnetite particles could be made by seed mediated process. In this process, the smaller Fe_3O_4 nanoparticles (as seeds) were mixed with more precursor materials and the mixture was treated similar procedure discussed above. By controlling the quantity of nanoparticle seed, Fe_3O_4 nanoparticles with variable sizes can be synthesized. For example, $Fe(acac)_3$ (2 mmol), 1,2-hexadecanediol (10 mmol), benzyl ether (20 mL), oleic acid (2 mmol), and oleylamine (2 mmol) were mixed and magnetically stirred under a flow of nitrogen. A 60 mg sample of 6 nm Fe_3O_4 nanoparticles dispersed in hexane (4 mL) was added. The mixture was first heated to 100 °C for 30 min to remove hexane, then to 200°C for 1 h. Under a blanket of nitrogen, the mixture was further heated to

reflux (~300 °C) for 30 min. The black-colored mixture was cooled to room temperature by removing the heat source. Following the separate procedures described in the synthesis of 4 nm particles, a black hexane dispersion of 8 nm Fe_3O_4 nanoparticles was produced. Similarly, 80 mg of 8 nm Fe_3O_4 seeds reacted with $Fe(acac)_3$ (2 mmol) and the hexadecanediol (10 mmol) led to 10 nm Fe_3O_4 nanoparticles, and so on.

Figure 3.1 is the representative TEM micrographs of as synthesized magnetite nanoparticles with different particle size. The overall size of the particle can be made ranging from 4nm to around 20nm. The magnetite particles are monodisperse and uniform based on the TEM results. Figure 3.2 show the results from X-ray diffraction (XRD) and select area electron diffraction (SAED) measurements, which further confirmed the phase structure of the magnetite particles. The diffraction rings on SAED pattern can be index with the XRD peaks, respectively. The figure 3.3 is the SQUID

hysteresis loops at 5 K and 300K. The curves reveal the magnetite particles are superparamagentic with quite high saturation magnetism.

Figure 3.1 TEM images of as-synthesized iron oxide nanoparticles with different particle size. 1A and 1B are representing small magnetite particles around 8 nm in size. 1C and 1D are representing large magnetite particles around 12-13 nm in size.

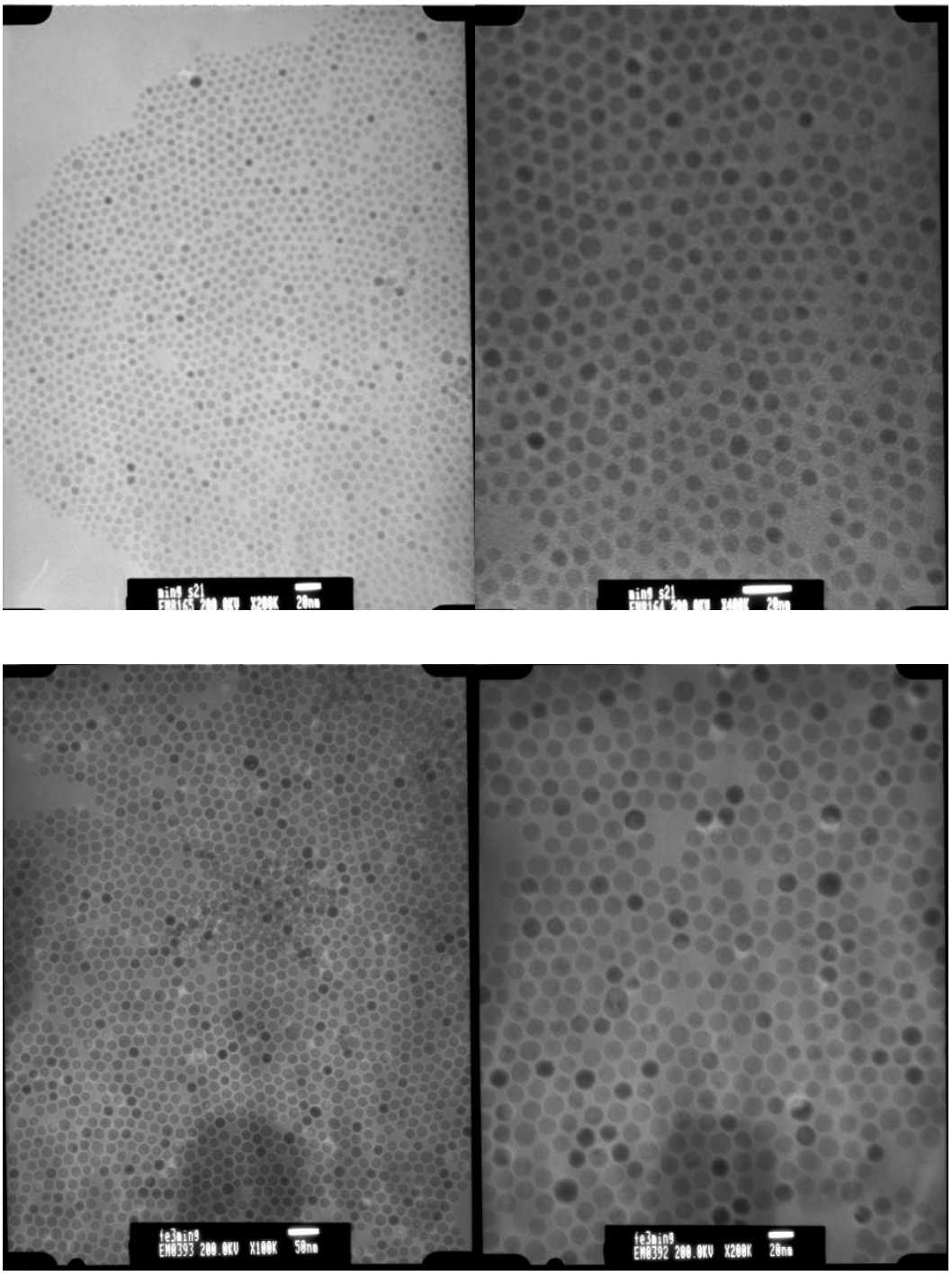

Figure 3.2 XRD and SAED of iron oxide nanoparticles. 2A is XRD pattern and 2B is SAED diffraction pattern. The diffraction ring in 2B (1, 2, 3, 4, 5, 6) can be indexed to XRD pattern (220), (311), (400), (422), (511) and (440). They do match the stardard spinel structure magnetite.

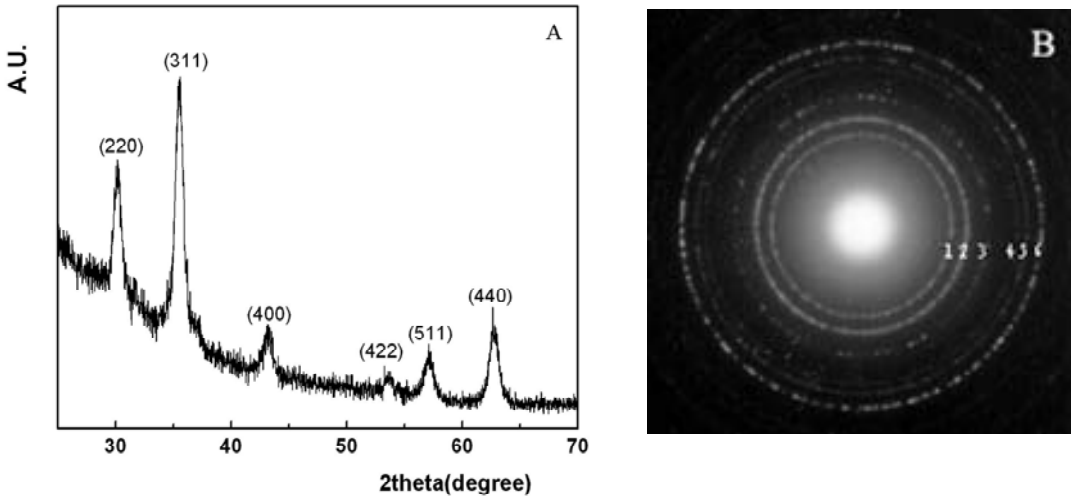

Figure 3.3 Magnetic hysteresis loops at 300 K and 5 K for representative iron oxide nanoparticles

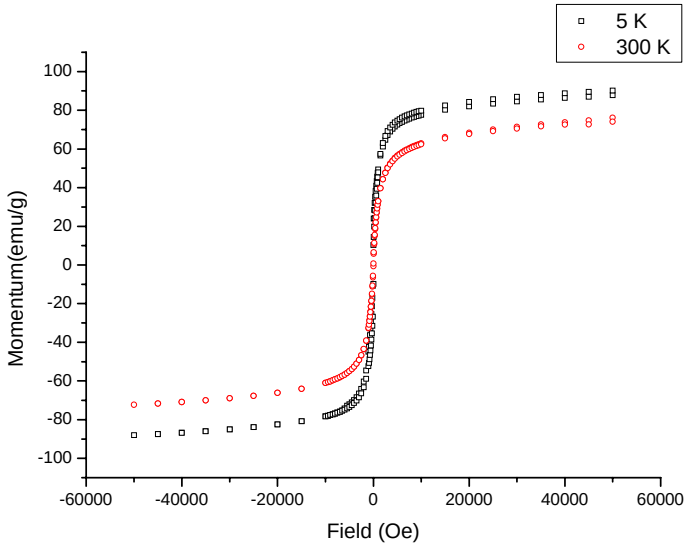

3.2.3 Indium Oxide nanoparticles

Indium oxide (In_2O_3) has been used widely for ultra-sensitive toxic gas (such as NO_2 and NH_3) detectors, transparent conductors, solar cells, and optoelectronic devices. In the last two decades, various types of indium oxide materials including thin films, nanowires and quantum dots have been intensively investigated. The In_2O_3 quantum dots have shown interesting photoluminescence properties and are good candidates for bio-labeling applications. [38-51]

We still use the high temperature solution approach to synthesize indium oxide nanoparticles and the high boiling point long chain hydrocarbon solvent hexadecane was selected. The general synthesis approach is as following: Indium acetate, oleic acid, oleylamine and hexadecane were mixed and magnetically stirred under nitrogen atmosphere. The mixture was vacuumed and heated to 110 ^{0}C for 30 minutes and then trimethylamine N-oxide was added to the mixture. The temperature of the reaction was increased to 120 ^{0}C and kept for additional 1 h. The mixture was quickly heated to reflux (~290 ^{0}C) for additional 1 h. The bright brown-colored mixture was cooled to room temperature quickly and collected by centrifugation after adding a sufficient amount of ethanol. By following the similar procedure discussed above, the precipitated particles were separate and re-dispersed in hexane with light yellow color and stored for later use.

In a typical experiment, 0.40 mmol of indium acetate (99.99%), 0.55 mL of oleylamine (70%), and 0.60 mL of oleic acid (90%) were combined with 8.0 mL of hexadecane (>99%) in a three-neck flask equipped with a condenser. The system was

vacuumed at room temperature and at 110 °C for 30 mins, respectively, to form a clear light-green solution. At 110°C, 1.45 mmol of trimethylamine *N*-oxide (TMNO, 98%) was introduced into this vigorously stirred hot mixture under an nitrogen atmosphere. The temperature of this mixture was then increased to 120 °C, where it remained for 1 h under agitation with nitrogen protection. The color of the solution gradually turned light yellow. The temperature was further increased to ~290 °C at a rate of 10 °C/min for an additional 35 min reflux. The mixture was clear-brown during the first few minutes at 290 °C, and subsequently changed to yellow precipitation during the following 20 min, and finally turned clear again. These colloids were cooled to room temperature by quickly removing the heating source, and then isolated by adding a sufficient amount of ethanol and separating with centrifugation. The yielded precipitate was redispersed in hexane followed by centrifugation to remove the very small amount of insoluble aggregates.

In this reaction condition, the around 8 nm indium oxide seeds can be made. With the seed mediated growth technique, larger size indium oxide particles up to 20 nm can also be synthesized.

Figure 3.4 is the representative TEM micrographs of as synthesized indium oxide nanoparticles with different particle size. The overall size of the particle can be made ranging from about 8nm to around 20nm. The indium oxide particles are monodisperse and uniform based on the TEM results. Figure 3.5 shows the results from X-ray diffraction (XRD) and figure 3.6 shows Energy Dispersive Spectroscopy (EDS) measurements, which further confirmed the phase structure and chemical composition of

the indium oxide particles. We also measured the photoluminescence properties of indium oxide nanoparticles which will be discussed in the later chapters.

Figure 3.4 TEM images of as-synthesized indium oxide nanoparticles with different particle size. 4A and 4B are small nanoparticles with 10 nm in size. 4C and 4D are large nanoparticles with about 20 nm in size.

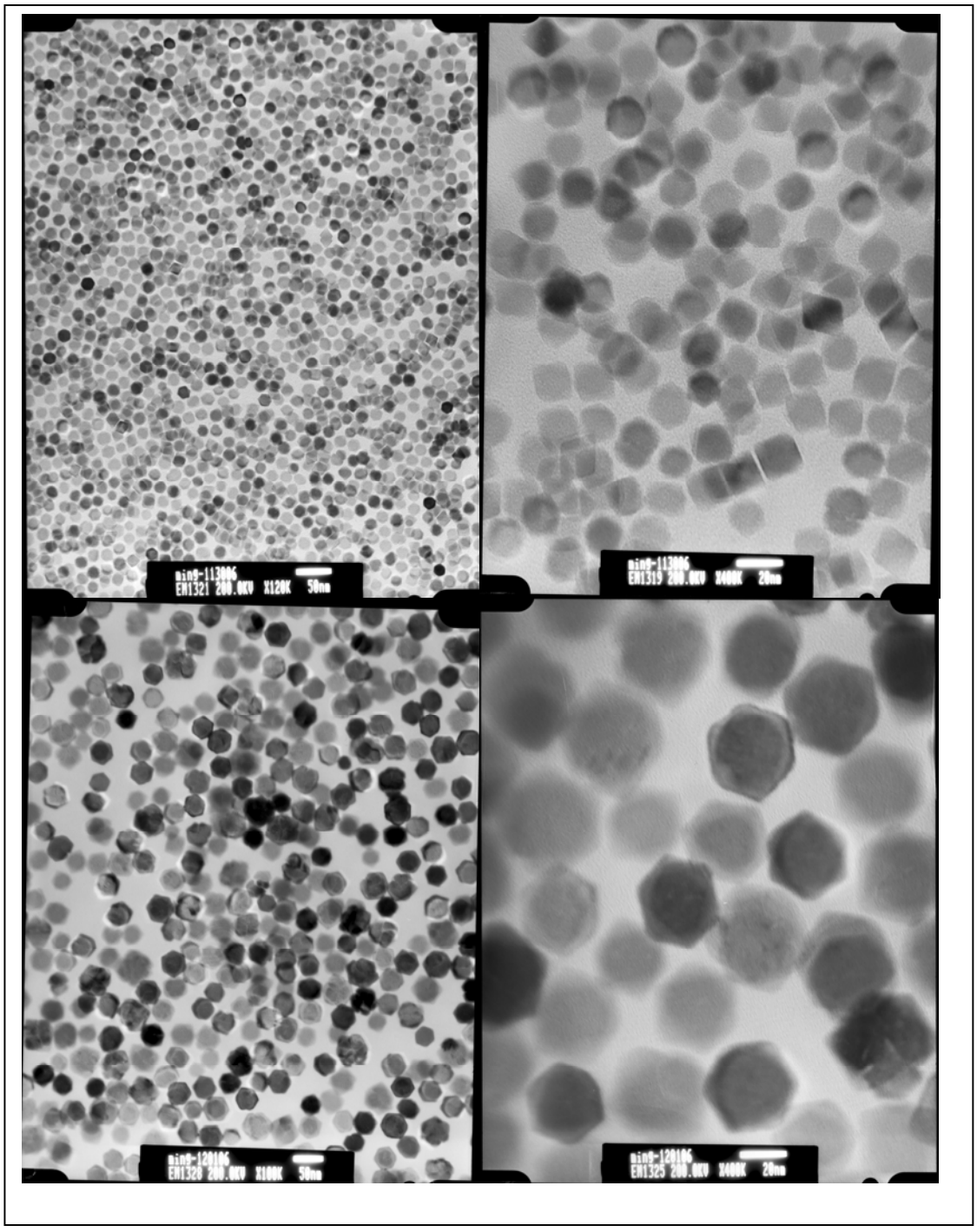

Figure 3.5 XRD of as-synthesized indium oxide nanoparticles and all the characteristic peaks are matching standard indium oxide.

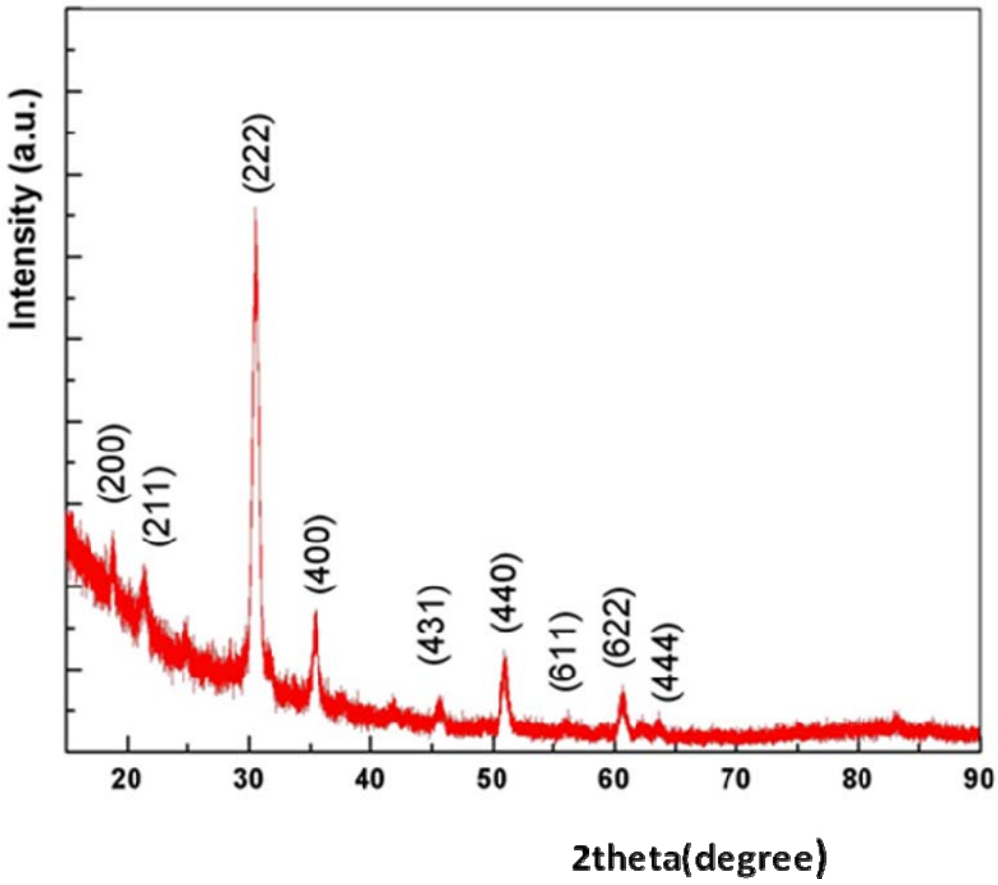

Figure 3.6 EDS of Indium oxide nanoparticles show the In presence.

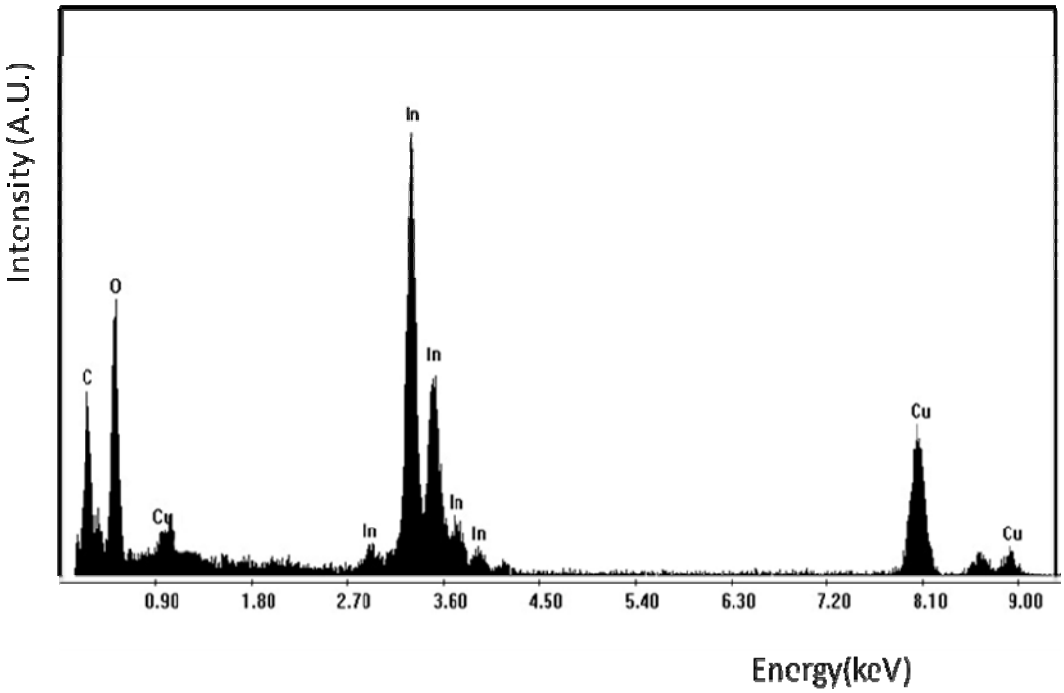

3.2.4 Size and Shape control [52-57]

Size and shape-controlled nanocrystals of metal oxide can be achieved by using this high temperature nonaqueous approach, which could lead to some unique properties and can potentially be employed in numerous applications.

We are synthesizing the larger metal oxide nanoparticle from the smaller seed particles and we have to well adjust the ratio of the seed particles and the precursor materials. If the amount of the seed particles are too much or less, the size distribution of the final product will dramatically increase. (Figure 3.7). So we have to well control the amount of the seed particles we added while the seed mediated growth process is undergoing. Another important reaction parameter is temperature. Because the reaction temperature is directly related to the nuclei formation rate, it will determine how much and how fast the nuclei formed, which will further control the particle size and shape.

The most important parameter to control the particle shape is the type and amount of the capping ligands. Generally, we could get the spherical particles by using one capping ligand and can get rods, wire structure by using two different kind of capping ligands with adjust ratio.

To produce mondisperse nanocrystals with high quality and tunable size and shape, it is significant to understand their formation process. Based on the literature report and our experiment experience, the particle formation mechanism might be the aggregation of the small particles during the Oswald ripening process. Due to the

complicacy of the colloid solution, it is impossible to explain every phenomenon by using a mechanism, but we could find some aggregation tread from the figure 3.8.

3.3 Summary and conclusions

We have successfully synthesized the Fe_3O_4 and In_2O_3 nanoparticles with tunable size and shape. The nanocrystal are monodisperse and trend to form the self-assembly structure in non-polar solvent.

Figure 3.7 Size distribution increase during the seed mediated growth. The small nanoparticles and large particles coexist in the solution.

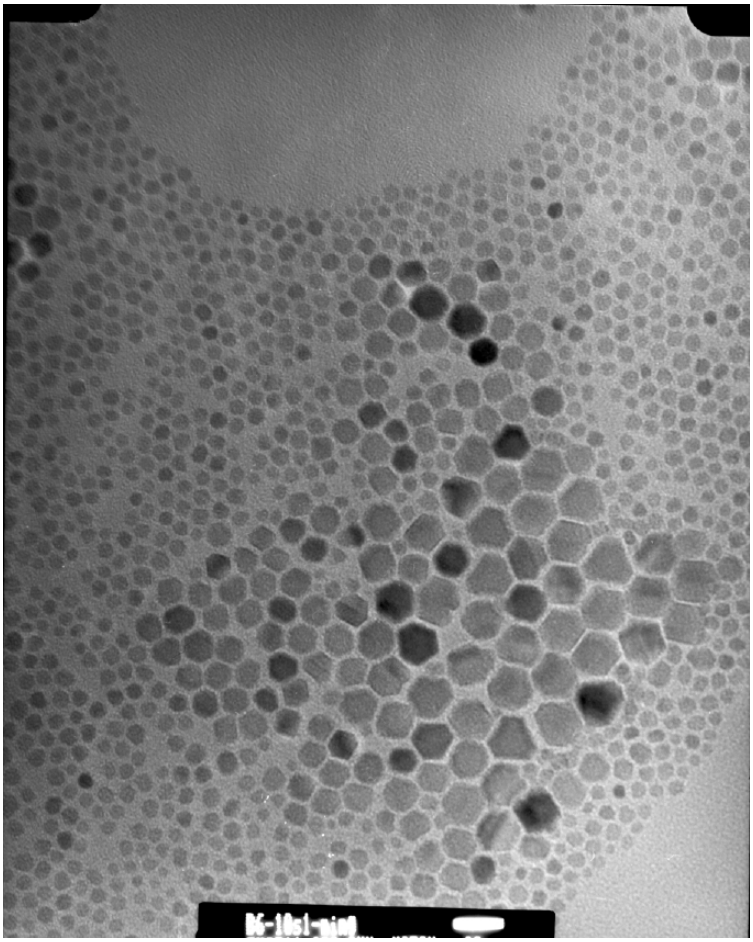

Figure 3.8 Small particles aggregate to form large particles. The intermediate step of the larger particle formation from the small particle clusters.

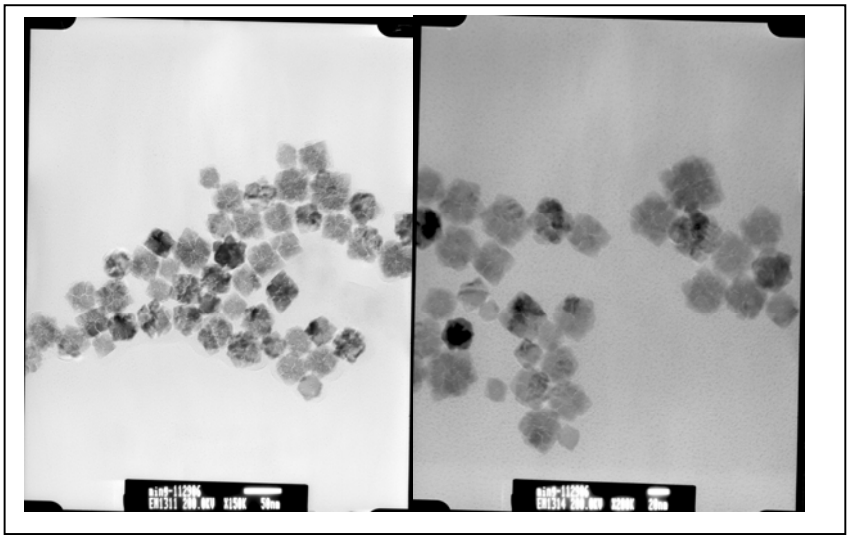

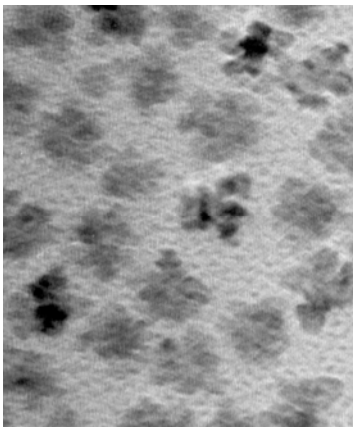

3.4 Reference

1. Niemeyer, C. M.; *Angew. Chem .Int. Edit*. **2001,** *40,* 4128-4158.
2. Mirkin, C. A. *MRS Bulletin,* **2000**, *25*, 43-54.
3. Pichot, C.; Taniguchi, T.; Delair, T.; Elaissari, A. *J. Disper. Sci . Tech.* **2003**. *24,* 423-437.
4. Bell, A. T. *Science* **2003,** *299,* 1688-1691.
5. Rolison, D. R. *Science.* **2003**, *299,* 1698-1701.
6. Zhong, C. J.; Maye, M. M. *Adv. Mater***. 2001**, *13,* 1507-1511.
7. Luo, J.; Maye, M. M.; Lou, Y. B.; Han, L.; Hepel, M.; Zhong, C. J. *Catalysis Today***. 2002**. *77 ,* 127-138.
8. Maye, M. M.; Lou, Y. B.; Zhong, C. J. *Langmuir* **2000**. *16,* 7520-7523.
9. Lou, Y.B.; Maye, M. M.; Han, L.; Luo, J.; Zhong, C. J. *Chem. Comm***. 2001.** , 473-474.
10. Barratt, G. *Cellular and Molecular life Sci***. 2003.** *60,* 21-37.
11. Leroux, J. C.; Allemann, E.; DeJaeghere, F.;Doelker, E.; Gurny, R. *J. Contr. Ralease.* **1996**. *39,* 339-350.
12. Brigger, I.; Dubernet, C.; Couvreur, P. *Adv. Drug Delivery Rev*. **2002**. *54*, 631-651.
13. Labhasetwar, V.; Song, C. X.; Levy, R. J. *Adv. Drug Delivery Rev***. 1997,** *24 ,* 63-85.

14. Choi, H.-J.; Johnson, J. C.; He, R.; Lee, S.-K.; Kim, F.; Pauzauskie, P.; Goldberger,J.; Saykally, R. J.; Yang, P.; *J. Phys. Chem. B*. ; **2003**; *107*, 8721-8725.

15. Huang, M.; Mao, S.; Feick, H.; Yan, H.; Wu, Y.; Kind, H.; Weber, E.; Russo, R.; Yang, P. *Science* **2001**, *292,* 1897-1899.

16. Johnson, J.; Yan, H.; Schaller, R.; Haber, L.; Saykally, R.; Yang, P. *J. Phys. Chem*. *B* **2001**, *105*, 11387- 11390.

17. Johnson, J.; Choi, H. J.; Knutsen, K. P.; Schaller, R. D.; Saykally, R. J.; Yang, P. *Nat. Mater.* **2002**, *1,* 106-110.

18. Banyai, L.; Koch, S. W. *Semiconductor Quantum Dots*. **1993**, World Scientific Singapore.

19. Lubert Stryer. Bichemistry. W. H. Freeman & Company, New York. **1981**, 1-7.

20. Alivisatos, A. P. *Science* **1996,** *271,* 933-937.

21. Meldrum, F. C.; Heywood, B. R.; Mann, S. *Science* **1992**, *257*, 522-523.

22. Tartaj, P.; Morales, M. P.; Gonzalez-Carreno, T.; Veintemills-Verdaguer, S.; Serna, C. T. *J. Magn. Magn. Mater*. **2005**, *290-291*, 28-34.

23. Willner, I.; Katz, E. *Angew. Chem., Int. Ed*., **2004**, *43*, 6042–6108.

24. Tanaka, T.; Matsunaga, T. *Anal. Chem.;* **2000**; *72*, 3518-3522.

25. Krizova, J.; Spanova, A.; Rittich, B.; Horak, D. *J. Chromatogr. A* **,2005**, *1064*, 247-253.

26. Tartaj, P.; Serna, C. J. *J. Am. Chem. Soc*. **2003**, *125*, 15754-15755.

27. del Monte, F.; Morales, M. P.; Levy, D.; Fernandez, A.; Ocana, M.; Roig, A.; Molins, E.; O'Grady, K.; Serna, C. J. *Langmuir* **1997**, *13*, 3627-3634.

28. Matsura, V.; Guari, Y.; Larionova, J.; Guérin, C.; Caneschi, A.; Sangregorio, C.; Lancelle-Beltran, E. ; Mehdi, A;. Corriu, R. J. P. *J. Mater. Chem.*, **2004**, *14*, 3026-3033.

29. Deng, Y.; Wang, C.; Hu, J.; Yang, W.; Fu, S. *Colloids and Surfaces A: Physicochem. Eng. Aspects* **2005,** *262*, 87–93.

30. Lu, A.-H.; Li, W.-C.; Kiefer, A.; Schmidt, W.; Bill, E.; Fink, G.. Schuth, F. *J. Am. Chem. Soc.* **2004**, *126*, 8616-8617.

31. Santra, S.; Tapec, R.; Theodoropoulou, N.; Dobson, J.; Hebard, A.; Tan, W. *Langmuir;* **2001**; *17*, 2900-2906.

32. Yang, H.-H.; Zhang, S.-Q.; Chen, X.-L.; Zhuang, Z.-X.; Xu, J.-G.; Wang, X.-R. *Anal. Chem.***2004**; *76*, 1316-1321.

33. Im, S. H.; Herricks, T.; Lee, Y. and Xia, Y., *Chem. Phys. Lett.* **2005**, *401*, 19-23.

34. Haddad, P. S; Duarte, E. L; Baptista, M.S; Goya, G. F; Leite, C; Itri, R. *Prog. Colloid. Polym. Sci.*; **2004**; *128*, 232-238.

35. Sun, S.; Zeng, H. *J. Am. Chem. Soc.* **2002**; *124*, 8204-8205.

36. Hyeon, T. *Chem. Commun.*, **2003**, 927-930.

37. Selvan, S. T.; Tan, T. T.; Ying, J. Y. *Advanced Materials* **2005**, *17*, 1620-1625.

38. Kim, J.; Lee, J. E.; Lee, J.; Yu, J. H.; Kim, B. C.; An, K.; Hwang, Y.; Shin, C.-H.; Park, J.-G.; Kim, J.; Hyeon, T. *J. Am. Chem. Soc.;* **2006**; *128,* 688-689

39. Darbandi, M.; Lu, W.; Fang, J.; Nann, T. *Langmuir;* **2006**; *22*, 4371-4375.

40. Cheng, G.X.; Shen, F.; Yang, L.F.; Ma, L.R.; Tang, Y.; Yao, K.D.; Sun, P.C. *Mater.Chem. Phys*. **1998**, *56*, 97-10.

41. S.A. Empedocles, D. J. Norris and M. G. Bawendi, *Phys. Rev. Lett*. **1996**, *77*, 3873.

42. A. P. Alivisatos, *J. Phys. Chem*. **1996**, *100*, 13226.

43. C. B. Murray, D. J. Norris and M. G. Bawendi, *J. Am. Chem. Soc.* **1993**, *115*, 8706.

44. M. Jr. Bruchez, M. Moronne, P. Gin, S. Weiss and A. P. Alivisatos, *Science,* **1998** *25*, 2013.

45. X. Gao, Y. Cui, R. M. Levenson, L. W. K. Chung and S. Nie, *Nature Biotech*. **2004**, *22*, 969.

46. L. Shi, V. De Paoli, N. Rosenzweig and Z. Rosenzweig*, J. Am. Chem. Soc*. **2006**, *128*, 10378.

47. D. Zhang, Z. Liu, C. Li, T. Tang, X. Liu, S. Han, B. Lei and C. Zhou, *Nano Letter* **2004**, *4*, 1919.

48. X. Li, M. W. Wanlass, T. A. Gessert, K. A. Emery and T. J. Coutts, *Applied Physics Letters* **1989**, *54*, 2674.

49. M. Liess, *Thin Solid Films* **2002**, *410*,183.

50. M. J. Zheng, L. D. Zhang, G. H. Li, X. Y. Zhang and X. F. Wang, *Applied Physics Letters*, **2001**, *79*, 839.

51. C. H. Liang, G. W. Meng, Y. Lei, F. Phillipp, and L. D. Zhang, *Advanced Materials,* **2001**, *13*, 1330.

52. A. Murali, A. Barve, V. J. Leppert, S. H. Risbud, I. M. Kennedy and H. W. H. Lee, *Nano Letter,* **2001**, *1*, 287.

53. Y. Zhao, Z. Zhang, Z. Wu and H. Dang, *Langmuir.* **2004**, *20*, 27.

54. W. S. Seo, H. H. Jo, K. Lee and J. T. Park, *Advanced Materials*, **2003**, *15*, 795.

55. Y. Lei and W.-K. Chim, *J. Am. Chem. Soc*. **2005**, *127,* 1487.

56. Q. Liu, W. Lu, A. Ma,; J. Tang, J. Lin and J. Fang, *J. Am. Chem. Soc*. **2005**, *127*, 5276.

Chapter 4 Synthesis of bimetal oxide nanoparticles

4.1 Introduction

We have already discussed the synthesis of metal oxide nanoparticles such as magnetite and Indium oxide with only one metal precursor in chapter 3. In this chapter, we will focus on the synthesis of bimetal oxide nanoparticles with more than one metal precursor. The $CoFe_2O_4$ and $LiCoO_2$ nanoparticles will be used as the examples to show the typical synthetic strategy. Furthermore, we will discuss the physical property of those nanoparticles as well.

4.1.1 $CoFe_2O_4$

Recently metal-oxide nanoparticles have been the subject of much interest because of their unusual optical, electronic and magnetic properties, which often differ from the bulk. Cobalt ferrite ($CoFe_2O_4$) nanoparticles are well-known material with very high cubic magnetocrystalline anisotropy, good coercivity, and moderate saturation magnetization. These properties, along with their great physical and chemical stability, make $CoFe_2O_4$ nanoparticles a promising material for magnetic recording applications such as audio and videotape and high-density digital recording disks etc. The magnetic character of the particles used for recording media depends crucially on the size, shape and purity of these nanoparticles. These particles should be single domain, pure phase, having high coercivity and medium magnetization. Hence the need for developing

fabrication processes that are relatively simple and yield controlled particle sizes draws greatly attention in recent years. [1-18]

For many applications synthesis of uniform-size nanoparticles is of key importance, because the magnetic properties depend strongly on their dimensions. Recently, great efforts have been made by various groups to achieve a fine-tuning of the size of cobalt ferrite nanoparticles employing different synthesis techniques and varying the experimental parameters such as heating rate, and quantity of surfactants. Kim and his coworkers prepared cobalt ferrite nanoparticles ranging from 2 to 14 nm by controlling co-precipitation temperature of Co^{2+} and Fe^{2+} ions in alkaline solution although the size distribution was pretty wide. Chinnasamy and his coworkers employed a modified oxidation process to synthesize cobalt ferrite particles with diameters ranging from a few micrometers to about 15 nm. Rajendrain and his colleagues demonstrated 6 to 20 nm sized cobalt ferrites prepared in aqueous solution at room temperature by the oxidative co-precipitation of Fe^{2+} and Co^{2+}. Morais and his corkers showed the size-controlled synthesis of the nanoparticles of 10 to15nm in aqueous solution at 95^{o}C by controlling stirring speed. Moumen and his coworkers used oil-in-water micelle to prepare size-controlled Cobalt ferrite in the range of 2 to 5 nm. Liu, Moomen, Pileni and several other groups also reported the nanoparticles of 2 to 35 nm in diameter which were prepared in normal micelle using different surfactants. Recently Sun, Murray and their coworkers synthesized cobalt ferrite nanoparticles with sizes variable from 4 to 20 nm in diameter by combining nonhydrolytic reaction with seed-mediated growth method.

Cobalt ferrite nanoparticles have been synthesized by a wide variety of methods as mentioned above. Although these methods are able to produce nano-sized ferrite particles, the quality of the nanoparticles is often poor. In many cases, a large size distribution is reported and size control is arbitrary. Compared with other methods used for preparing ferrites nanoparticles, the chemical solution method which we have discussed in the previous has its unique advantages in producing small particles size (down to 4 nm) with very narrow size distribution, as well as good crystallinity and stability. [19-27]

4.1.2 $LiCoO_2$

Li-ion cells consisting of $LiMeO_2$ (Me: a 3d-transtion metal element) and carbon materials have been of interest because of their capability to be safely operated for thousands of cycles while retaining a high energy density. Materials with the above formula more exrensively examined for the positive electrodes include $LiCoO_2$, $LiNiO_2$, $LiCo_{1-x}Ni_xO_2$ and $LiMnO_2$. Among these cathode materials, more research has been done on LiCoO2 because of its high energy density and good cycling performance. LiCoO2 has served as an archetypal cathode material for secondary Lithium batteries ever since the discovery by Mizushima and his colleges that Li ion can be reversibly removed (deintercalated) from and reinserted (intercalated) into Li_XCoO_2. The layered form of LiCoO2, which has a homobohedral symmetry belonging to the space group R-3m, is ideally suited to accommodate large changes of Li content. This crystal structure consists of close-packed oxygen layers stacked in an ABCABC sequence with Co and Li ions residing in octahedral sites in alternating layers between the oxygen planes.

Lithium cobalt oxide exhibits many of the essential properties required for a reliable cathode material. The voltage of Li_xCoO_2 is sufficiently high to guarantee a high energy density, although it is not too high to cause electrolyte decomposition. In addition to its favorable electrochemical properties, $LiCoO_2$ also exhibits phase transformations that are typical of many intercalation compounds.

$LiCoO_2$ with layer structure has been used as a cathode material in lithium batteries. Recently, it is found that the nanostructured $LiCoO_2$ powders exhibit an enhanced electrochemical performance compared to their bulk phase. Physiochemical properties of the nanocrystalline $LiCoO_2$ powders like crystallite size, homogeneity, chemical stability are mainly depending on the synthesis process. A number of wet chemical routes were investigated for the synthesis of nanocrystalline metal oxides. But the solid state approaches still dominate the synthesis of $LiCoO_2$ powders. In this chapter, we will introduce our wet chemistry method to the preparation of $LiCoO_2$ nano-size powders. And we will discuss the size-control and shape-control by adjusting the reaction parameters. [28-31]

4.2 Experiment

4.2.1 Experimental Procedure for Synthesis of $CoFe_2O_4$ Nanoparticles

The synthesis was carried out using standard airless process. The reagents were obtained from commercial sources and used without further purification. The process involves simultaneous chemical decomposition of cobalt (II) acetylacetonate $Co(acac)_2$

and iron (III) acetylacetonate $Fe(acac)_3$ at high temperature in nonpolar solution phase. Particle diameter was tuned from 4 nm to 20 nm by varying reaction conditions and by seed-mediated growth method.

4.2.1.1 Synthesis of 4 nm and 6 nm $CoFe_2O_4$ Nanoparticles seeds

In the case of 4 nm particles the composition was controlled by varying the mole ratios of the precursors $Fe(acac)_3$ and $Co(acac)_2$ used during the chemical synthesis. Typically, Fe $(acac)_3$ (2 mmol), $Co(acac)_2$ (1 mmol), 1,2-hexadecanediol (10 mmol), oleic acid (4 mmol), oleyl amine (4 mmol), and phenyl ether (20 ml) were mixed and magnetically stirred under a flow of nitrogen for 30 minutes. The flask was then heated to 100^0C and held for 20 min. During this hold, 4 mmol of oleylamine and 4 mmol of oleic acid were injected into the flask while continuing the nitrogen purge. After the 20 min hold, the mixture was maintained under a nitrogen blanket and heated to 200^0C and held for 20 minutes and then heated to 265^0C at a rate of approximately 10^0C per minute. The flask was maintained at the refluxing temperature of 265^0C for 30 min before it was cooled down to room temperature under the nitrogen blanket. Afterward, all procedure was performed open to the atmosphere.

Purification of the nanoparticles was accomplished as follows: 5 ml of the dispersion taken from the flask was added to 20 ml of ethyl alcohol (ethanol) and the mixture was centrifuged at 4000 rpm for 15 min. The supernatant was discarded and the precipitate redispersed in 10 ml of hexane and 1~2 ml of ethanol. Additional small amount of oleylamine and oleic acid is added to aid in redispersing the nanoparticles.

This dispersion was centrifuged at 4000 rpm for 15 min. The supernatant was transferred to a new centrifuge tube, and any precipitate was discarded. An additional 15~20 ml of ethanol was added to this dispersion and centrifuged again. The supernatant was discarded and the remaining dark red-brown precipitate was re-dispersed in hexane to form 4 nm $CoFe_2O_4$ nanoparticles. The 6 nm particles were prepared by replacing phenyl ether with benzyl ether and following the similar procedure discussed above.

4.2.1.2 Synthesis of larger $CoFe_2O_4$ Nanoparticles by seed mediated growth

Mole ratios of 2:1 of $Fe(acac)_3$ and $Co(acac)_2$ was kept constant to prepare larger particles by seed mediated growth method using the 4 nm and 6 nm as seeds. In this process, the smaller $CoFe_2O_4$ nanoparticles (as seeds) were mixed with more precursor materials and the mixture was treated similar procedure discussed above. By controlling the quantity of nanoparticle seed, $CoFe_2O_4$ nanoparticles with various sizes can be synthesized. For example, mixing and heating 60 mg 4 nm $CoFe_2O_4$ particles with 2 mmol of $Fe(acac)_3$, 1 mmol of $Co(acac)_2$, 8 mmol of 1, 2-hexadecanediol, 2 mmol of oleic acid, and 2 mmol of oleylamine formed 8 nm CoFe2O4 particles. Similarly, mixing and heating 50 mg of 8 nm $CoFe_2O_4$ seed particles with 2 mmol of Fe(acac)3, 1 mmol Co(acac)2 , 8 mmol of 1, 2-hexadecanediol, 2 mmol of oleic acid, and 2 mmol of oleylamine formed 12 nm $CoFe_2O_4$ particles. Using this seed-mediated growth approach, larger nanoparticles of $CoFe_2O_4$ up to 20 nm could be made.

4.2.2 Experimental Procedure for Synthesis of $LiCoO_2$ Nanoparticles

The synthesis was carried out using standard airless process. The reagents were obtained from commercial sources and used without further purification. The process involves simultaneous chemical decomposition of Lithium acetate and Cobalt (III) acetate at high temperature in nonpolar solution hexadecane. Particles size was tuned from 8 nm to 15nm by varying reaction conditions and by seed-mediated growth method. By adjusting the ratio of the capping ligands, the different shape of the LiCoO2 nanocrystal can also be achieved.

4.2.2.1 Synthesis of 8 nm $LiCoO_2$ spherical Nanoparticles

In a typical experiment, 0.4mmol Cobalt acetate, 0.2mmol Lithium acetate, 0.55 ml of oleylamine (70%) and 0.60 ml of oleic acid (90%) were combined with 7.0 ml of hexadecane (>99%) in a three-neck flask equipped with a condenser. The mixture was vacuumed at room temperature and at 110^0C for 30 minutes respectively to form a clear dark-blue solution. At temperature 110^0C, 1.45mmol of trimethylamine N-oxide (TMNO, (98%) was subsequently introduced into this vigorously stirred hot mixture under an nitrogen blanket. The temperature of this system was then increased to 160^0C, where it remained for one hour under agitation with nitrogen protection. The color of the solution gradually turned black. The temperature was further increased to 290^0C at a heating rate of 10^0C/min for an additional 35 minutes reflux. The colloid solution was cooled to room temperature by removing the heating source, and then followed the similar procedure discussed above to isolate the nanoparticles by adding a sufficient amount of ethanol and separating with centrifugation. The final product was re-dispersed in hexane after removing the very small amount of insoluble aggregates. By using seed-mediated growth approach discussed above, the larger $LiCoO_2$ particles can also be made.

4.2.2.2 Synthesis of 10 nm $LiCoO_2$ cubic Nanoparticles

The ratio of the capping ligands is the key to synthesize the cubic nanoparticles. In a typical synthesis, 0.4mmol Cobalt acetate, 0.2mmol Lithium acetate, 3.5 ml of oleylamine (70%) and 0.60 ml of oleic acid (90%) were combined with 7.0 ml of hexadecane (>99%) in a three-neck flask equipped with a condenser. The mixture was vacuumed at room temperature and at 110^0C for 30 minutes respectively to form a clear dark-blue solution. At temperature 110^0C, 1.45mmol of trimethylamine N-oxide (TMNO, (98%) was subsequently introduced into this vigorously stirred hot mixture under an nitrogen blanket. The temperature of this system was then increased to 160^0C, where it remained for 1hour under agitation with nitrogen protection. The color of the solution gradually turned black-green. The temperature was further increased to 290^0C at a heating rate of 10^0C/min for an additional 35 minutes reflux. 2 ml oleic acid was injected to the system, and then the colloid solution was cooled to room temperature by removing the heating source. The final particles were re-dispersed in hexane solution in black brown color for further analysis.

4.3 Results and Discussion

The nanoparticles were characterized by TEM, XRD, ICP, SQUID and optical measurement.

4.3.1 $CoFe_2O_4$

TEM analysis shows that $CoFe_2O_4$ nanoparticles as-synthesized in first step and prepared by seed-mediated method are monodisperse. Figure 4.1 show typical TEM

Figure 4.1 TEM micrographs of different size cobalt iron oxide nanoparticles. The particle sizes are 4 nm, 6 nm, 8 nm and 10 nm, respectively.

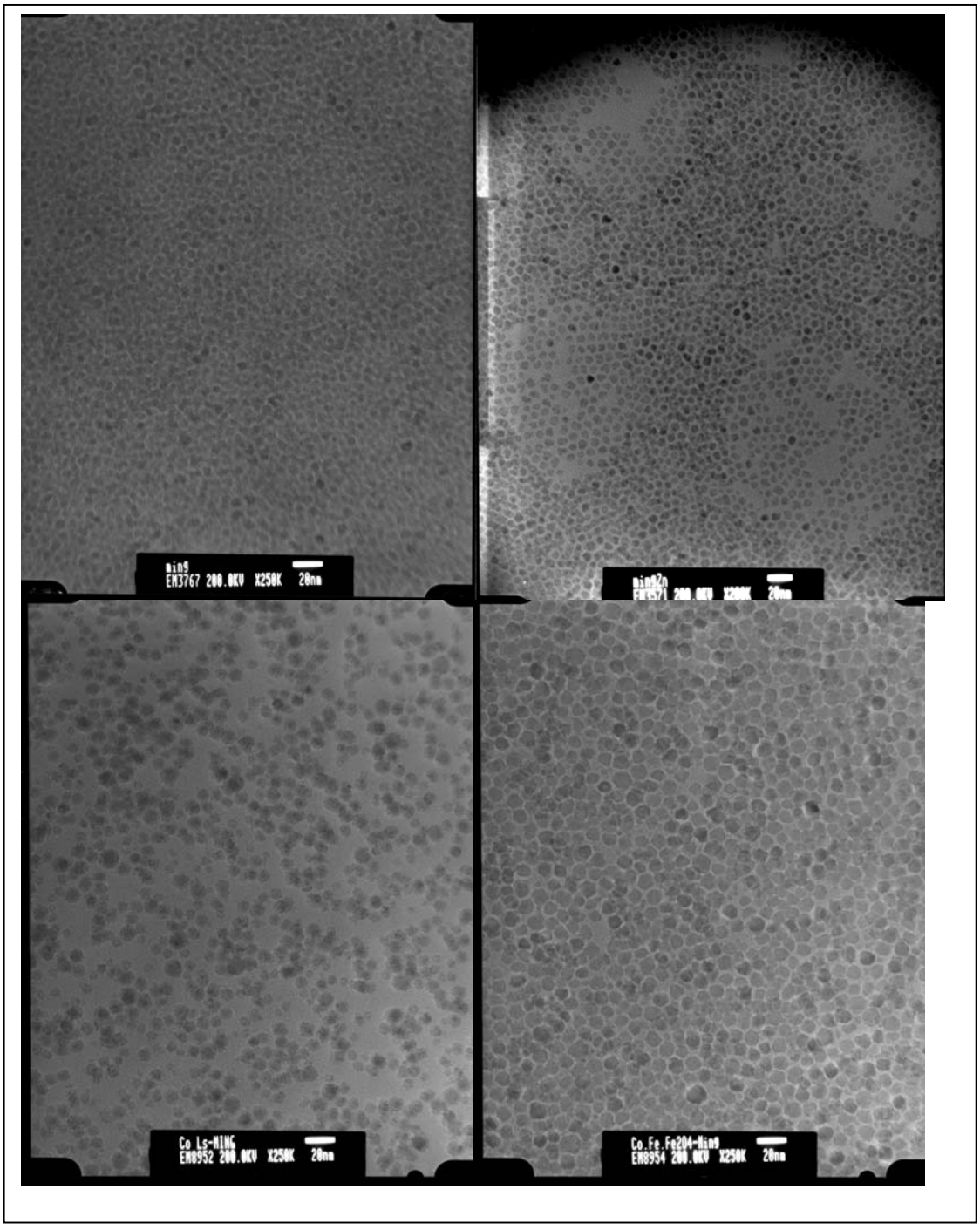

images of different size $CoFe_2O_4$ nanoparticles deposited on TEM carbon-coated copper grid from their hexane dispersion and dried at room temperature. It can be seen from the TEM images that the particles have a narrow size distribution and uniform size. From the synthesis of variable size cobalt ferrite, we can further confirm our synthetic route could be used widely for different type metal oxides nanocrystals.

4.3.2 $LiCoO_2$

The composition of as-synthesized $LiCoO_2$ nanoparticles was determined by using ICP method because EDS cannot detect the lithium element. The ICP result show that average composition of Li ion to Co iron is around 1:1 by atomic percentage.

The shape of Lithium cobalt oxide nanoparticles can be controlled by adjusting reaction parameter. We believed the ratio of the capping ligands was the most important parameter to affect the particle shape. With the ratio of oleylamine to oleic acid as 5~6, the cubic particles were achieved. If the ration is close to 1, we only can get the spherical particles. The figure 4.2 shows the representative as-synthesized cubic-like $LiCoO_2$ particles with uniform size and trend to self-assemble on the carbon grids.

Figure 4.2 Cubic-like $LiCoO_2$ nanoparticles. The particle size is 10nm from two edges. The SAED result also shows the textile growth.

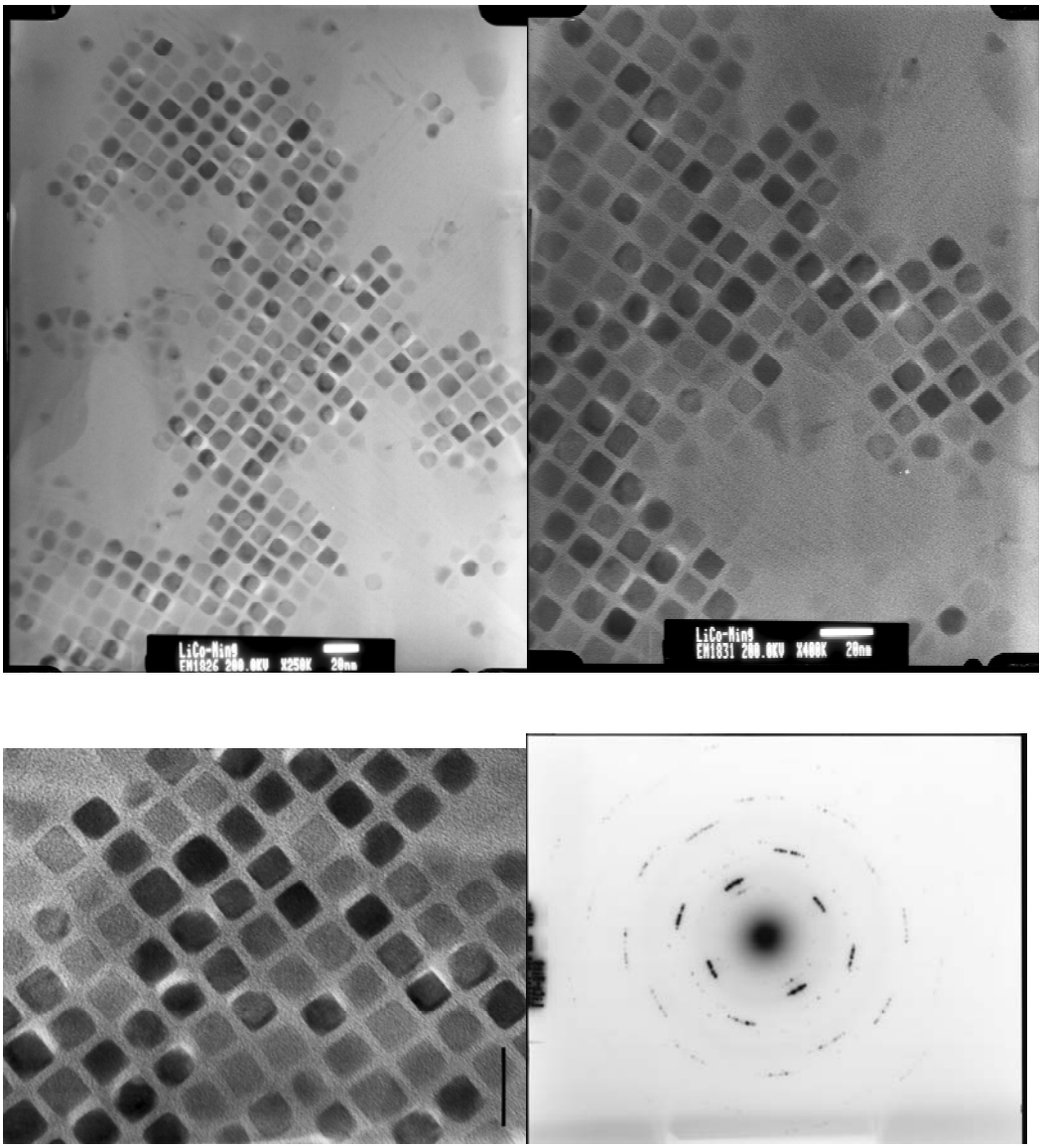

4.4 Summary and conclusions

We have successfully extended the high temperature nonaqueous solution method to the system with more than one metal precursor. Further experiments confirm this method is versatile for the metal oxide nanoparticles synthesis and allows good control over the crystal size and shape.

4.5 Reference

1. Soshin Chikasumi, "*Physics of Magnetism*" **1964**, John Wiley and Sons.
2. B. D. Cullity, "*Introduction to Magnetic Materials*", **1972**, Addison-Wesley Publishing.
3. Nicola A. Spaldn, "*Magnetic Materials: Fundamentals and Device Applications*", **2003**, Cambridge University Press
4. William D. Callister, Jr., "*Material Science and Engineering: An Introduction*", **2000**, John Wiley & Sons.
5. Robert C. O' Handley, "*Modern Magnetic Materials: Principles and Applications*", **2000**, Wiley & Sons.
6. J.C. Anderson, "*Magnetism and Magnetic Materials*", **1968**, Chapman and Hall Ltd.
7. J. M. D. Coey, *Journal of Alloys and Compounds*, **2000**, *326*, 2.
8. J. M. D. Coey, *Solid State Communications*, **1997**, *102*, 101.
9. E.F. Kneller, and V.R. Hawing*, IEEE Transactions on Magnetics*, **1991**, *27*, 3588.

10. R. Skomski, J.M.D. Coey,. *Physical. Review B*, **1993**, *48*, 15812.

11. Hao Zeng, Jing Li, J.P. Liu, Zhoung L. Wang, and Shouheng Sun, *Nature*, **2002**, *420*,395.

12. Im, S. H.; Herricks, T.; Lee, Y. and Xia, Y., *Chem. Phys. Lett.* **2005**, *401*, 19-23.

13. J. Sort, S. Surmach, J. S. Munoz, and M. D. Baro, *Physical Review B*, **2002**, *65*, 174420.

14. D.C. Jiles, *Acta Meterialia*, **2003**, *15*, 5907.

15. Eric E. Fullerton, J. S. Jiang, S. D. Bader, *Journal of Magnetism and Magnetic Materials*, **1999**, *200*, 392.

16. R. Skomski and J.M.D Coey, *IEEE Transactions on Magnetics*, **1994**, *30*, 607.

17. Kenneth J. Klabunde, "*Nanoscale Materials in Chemistry*", **2001**, John & Sons, Inc.

18. D. Goll and H. Kronmuller, *Naturwissenschaften*, **2000**, *87*,423.

19. Catherine C. Berry and Adam S. G. Curtis, Journal of Physics. D: *Applied Physics,* **2003**, *36*, 198.

20. Taeghwan Hyeon, *Chemical communication*, **2003**, 927.

21. M. Chastellain1, A. Petri1, M. Hofmann and H. Hofmann, *European Cells and Materials,* **2002**, *3*, 11.

22. D.K. Kim W. Voit, W. Zapka, B. Bjelke, M. Muhammed, and K.V. Rao, *Material Research Society Symp. Proc.* **2001**, 676**.**

23. M. A. Willard, L.K. Kulrihara, E.E. Carpenter, S. Calvin and V.G. Harris, *International Material Reviews*, **2004**, *49*, 3.

24. L. Fu, V.P. Dravid, K. Klug, X. Liu and C.A. Mirkin, *European Cell and Materials*, **2002**, *3*, 156.

25. CA Ross, *Annual Review of Material Research*, **2001**, *31*, 203.

26. S. Okamoto, O. Kitkami, N. Kickuchi, T. Miyazaki, and Y. Shimada, *Physical Review B*, **2003**, *67*, 94422.

27. D. Weller, M. F. Doerner, *Annual review of materials science*, **2000**, *30*, 611.

CHAPTER 5 SYNTHESIS OF SILICA COATED METAL OXIDE NANOPARTICLES IN MICROEMULSION SYSTEM

5.1 Introduction

Silica-coated colloidal particles are a class of materials widely used in many fields of colloid and materials science. A wide variety of coating procedures has been developed for these samples. These surface coatings allow manipulation of the interaction potential and make it possible to disperse colloids in a wide range of solvents from very polar to a polar. The so-called Stober growth1 of silica shells by addition of tetraethoxysilane to solutions of seed particles in an ethanol/ammonia mixture yields smooth surfaces since the growth takes place on a molecular scale. If silica-coated particles are grown further by this procedure, the polydispersity of the particles decreases with R^{-1}, where R is the particle radius. This makes it possible to grow crystals of core shell particles even when the cores are polydisperse. Silica colloids and silica-coated particles are often used as model particles to study phase behavior and diffusion. Surface modifications of silica spheres have yielded systems with hard-core potentials, short-range attractive potentials, and Yukawa potentials. In addition, the silica layer allows for controlled placement of various dyes. Such dye-labeled particles can be used in quantitative real-space studies with confocal fluorescence microscopy or as tracer particles in, for example, fluorescence recovery after photobleaching (FRAP) or time-resolved phosphorescence anisotropy measurements. [1-12]

Moreover, the possibility of the placement of dye molecules with nanometer precision allows the study of the local density of states in photonic applications. Interest in the use of silica-coated particles as building blocks for photonic crystals is increasing. Here the outer silica shell allows tuning of not only the interaction potential of the particles but also the optical properties of the crystal. An outer silica coating also offers new possibilities for the shape control of a particle. Silica particles can be anisotropically deformed in a controlled way by ion beam irradiation. This method was successfully applied to silica-coated gold particles. Due to deformation of the silica shell it was possible to deform spherical gold particles into silica colloids in a controlled way, while normally gold particles remain unchanged under these conditions. There are many surfaces that can be directly coated with silica because of the significant chemical affinity of these materials, like clay minerals, hematite, zirconia, and titania.

However, many other surfaces can only be coated with the help of stabilizers, surfactants, silane coupling agents, or a fast precipitation from a water glass solution, and most of these coating methods are multistep processes. For instance, in procedures using mercapto- or aminosilanes as coupling agent gold colloids, silver colloids, and semiconductor nanocrystals could be coated with silica. A critical step in many silica-coating procedures is the transfer of colloids that are only stable in aqueous solution to ethanol where the classical Stober process is performed. A widely used technique to achieve this transfer is the water glass process. First, colloidal particles are covered with a thin layer of sodium silicate in aqueous solution. If the particles are then sufficiently stabilized, they can be transferred into ethanol and be further coated with a thicker silica

layer using seeded growth. In this way nanoclusters could be coated with silica via a three step coating procedure. Such a step was also necessary for the coating of gold and silver colloids via the use of silane coupling agents. A disadvantage of this method is that the growth of the initial shell with sodium silicate is strongly pH dependent and not very well controllable.

Various methods for the coating of different colloids with silica can be found in the literature. The classical Stober synthesis (base-catalyzed hydrolysis of tetraalkoxysilane-precursors with subsequent condensation of these hydrolyzed species and its derivatives) has been used for silica coating of different kinds of colloidal particles. Liz-Marzan, Mulvaney, and co-workers have extensively studied metal-silica core-shell particles prepared by a liquid-phase procedure in which the use of a surface primer (a silane coupling agent) was necessary to provide the surface with silanol anchor groups. Rogach et al. also introduced a method of adding mercaptopropyltrimethoxysilane (MPS) as a coupling agent to incorporate semiconductor nanocrystals into silica. Major disadvantages of the Stober-based methods are the high requirements on purity of the reactants, the difficulty and multiplicity of the preparation steps, and the fact that it is not possible to directly coat nanoparticles with nonpolar ligands. The water-in-oil (W/O) microemulsion system in conjunction with the Stober synthesis and silane coupling method has been used for the preparation of silica-coated, metallic, magnetic and semiconductor nanocrystals.[28-30] In contrast to a previously published Stober-based method, the procedure is very robust against slight changes in the reaction parameters and the purity of reactants, and it does not need any surface modification and pretreatment.

Furthermore, it can be easily scaled-up, and no purification steps are required during the preparation of silica shell.

Guided by these considerations mentioned above and regarding that it is desirable in view of industrial applications to coat the nanoparticles by a more convenient method, we demonstrate a simple method by which monodisperse silica coated metal oxide particles can be prepared using a water in- oil (W/O) microemulsion containing Igepal CO-520 (see Chemicals, below), cyclohexane and water system. In this chapter, we report the details of this synthesis approach. The procedure yields nanocrystals encapsulated in a silica shell with a thickness tunable ranging from 2nm to 100 nm. Also the morphology and material property of nanocomposite will be discussed as well.

5.2 Experiments and results

Chemicals. Iron (III) acetylacetonate, 1,2-hexadecanediol, oleic acid, oleylamine and benzyl ether, Indium acetate, hexadecane, TMNO cyclohexane, polyoxyethylene(5)nonylphenyl ether (Igepal CO-520) and ammonium hydroxide (28-30%), tetraethylorthosilicate (TEOS) were purchased from Aldrich. All chemicals and solvents were used as received without additional purification.

5.2.1 Synthesis of silica coated magnetite nanoparticles

Strategies to prepare silica-coated magnetic nanoparticles are mainly based on a two-step process. The first step is to synthesize the magnetic particles in an organic solvent. Iron (III) acetylacetonate, 1,2-hexadecanediol, oleic acid, oleylamine and benzyl ether were mixed and magnetically stirred under argon atmosphere. The mixture was heated to 200 °C for 2 h and then heated to reflux (~295 °C) for 1 h. The black-colored mixture was cooled to room temperature and collected by centrifugation after diluting the sample with ethanol. The oleic acid stabilized magnetic particles were re-dispersed in hexane and used as precursors for seed-mediated growth. The second step is to apply the thin silica shell in a reverse microemulsion (scheme 5.1). After transferring the magnetic particles to cyclohexane, polyoxyethylene(5)nonylphenyl ether (Igepal CO-520) and ammonium hydroxide (28-30%) were added to form a brown transparent reverse microemulsion solution with the aid of a sonicator. Then, tetraethylorthosilicate (TEOS) was added and gently stirred for 48 h at room temperature. The reaction mixture was washed with methanol to remove the surfactant and collected by both magnetic separation and centrifugation. For SQUID and XRD analyses, the ethanol-dispersed magnetic-silica particles were dried in oven for overnight at 50 °C. [13-28]

TEM images of magnetite particles and silica coated magnetite particles are shown in Figure 5.1. Figure 5.1a shows a representative TEM image of as-synthesized Fe_3O_4 magnetic particles that were stabilized by oleic acid and can be dispersed very well in a hexane solution. The average size was around 8 - 10 nm. Figures 1b and 1c show ultra-thin silica-coated magnetic nanoparticles dispersed in ethanol. Although the size

distribution of the particles appears to broaden in figure 5.1b and 1c during the process of silica coating, the thin silica shell is readily apparent; the thickness of the silica was reasonably uniform at ~2 nm. It can be clearly seen that with a ~2 nm silica shell there are almost no bare magnetite and core-free silica nanoparticles, which can significantly improve the saturation magnetization of silica coated nanocomposites. This ultra-thin silica layer is very stable and robust and sufficient to protect the magnetite core from agglomeration and decomposition. We also can synthesis thicker silica shell magnetite nanoparticle (up to 100nm) by adjusting the reaction agents. The silica shell appears very uniform in thickness at about 20nm and quite smooth in surface morphology (figure 5.1d and 5.1e); However, the possibility to form multiple cores composite and pure silica particles increase when the silica shell gets thicker.

XRD measurements confirmed the presence of silica as the shell of the nanocomposite. Figure 5.2a, 5.2b exhibits the XRD spectra of Fe_3O_4 nanoparticles and Fe_3O_4@SiO_2 nanocomposite, respectively. Both XRD patterns are in good agreement with that of standard Fe_3O_4 with diffraction peaks of {220}, {311}, {400}, {422}, {511}, and {440}. The amorphous silica shell can be observed in Fe_3O_4@SiO_2 nanocomposite XRD pattern as well as the magnetite characteristic.

Magnetic properties of the ultra-thin shell magnetite-silica composite were characterized by SQUID magnetometry. The Fe_3O_4@SiO_2 particles are superparamagnetic at room temperature and hysteretic at 5K. Figure 5.3a shows the hysteresis loops, measured at 300 K and 5 K respectively. Zero field cooled-field cooled (ZFC-FC) thermal magnetization curves reveal that the blocking temperature (T_B) of Fe_3O_4@SiO_2 particles is approximately 133 K (figure 5.3b). Many bioapplications such

as cell separation or drug delivery require immediate magnetic attractions between particles and the external field. To meet this requirement, the particles should be superparamagnetic with highest possible saturated magnetization and fairly low blocking temperature. Due to the very thin silica shell, the saturation magnetization (M_S) of the Fe_3O_4@silica nanocomposite is around 15emu/g, which is a significant improvement over the values previously reported in the literature that generally is below 5emu/g.[12,13] Rossi and her coworker also reported the silica coated magnetic nanoparticles with the saturation magnetization of 13emu/g. However, with their method it is hard to stabilize the magnetic particles against aggregation, and the microemulsion method will allow better control to achieve the single magnetic core encapsuled in silica particles.[22] And the low blocking temperature enables our particles to be used over a wide temperature range. Those advantages open the possibility of easily manipulating these nanocomposites with magnetic fields. Generally the saturated magnetization of the nanocomposite decreases as the thickness of the silica shell increases. For example, the saturation magnetization with silica shell around 20nm drops to 1.5-2 emu/g. We believe the ultra-thin silica layer is sufficient to prevent the aggregation and decomposition of magnetic particles. Furthermore, silica has proven to be a good agent to conjugate to bio-molecular species; the possibility now exists to apply these nanocomposites as magnetic drug-delivery agents.

Scheme 5.1. Synthesis of Silica coated magnetite nanoparticle.

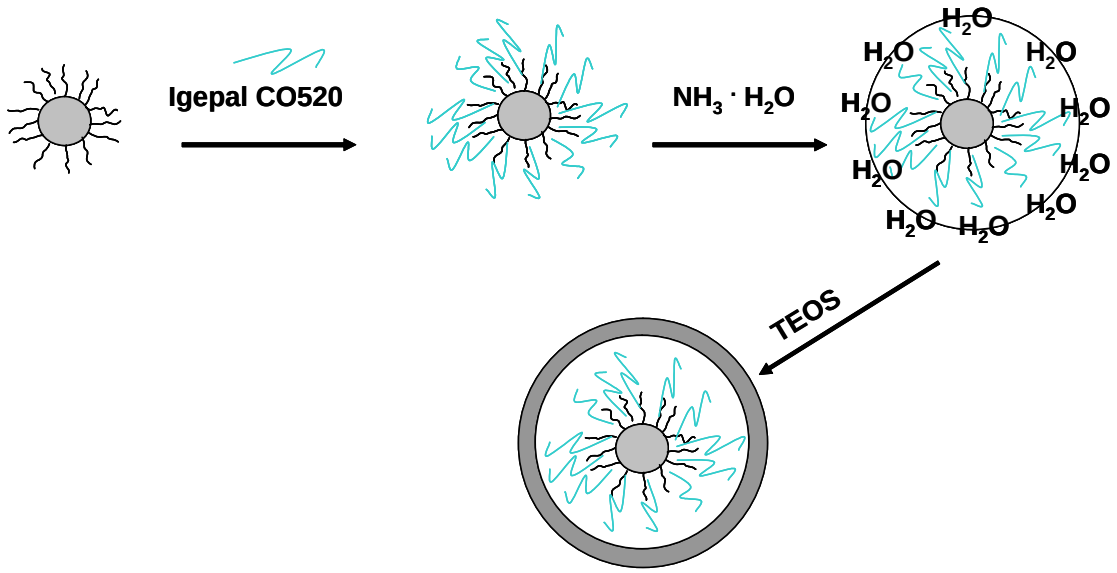

Figure 5.1. TEM micrograph of (a) as-synthesized Fe_3O_4 magnetic particles, (b,c) Fe_3O_4@SiO_2 (with the shell thickness of about 2nm), (d,e) Fe_3O_4@SiO_2 (the shell thickness of about 20 nm)

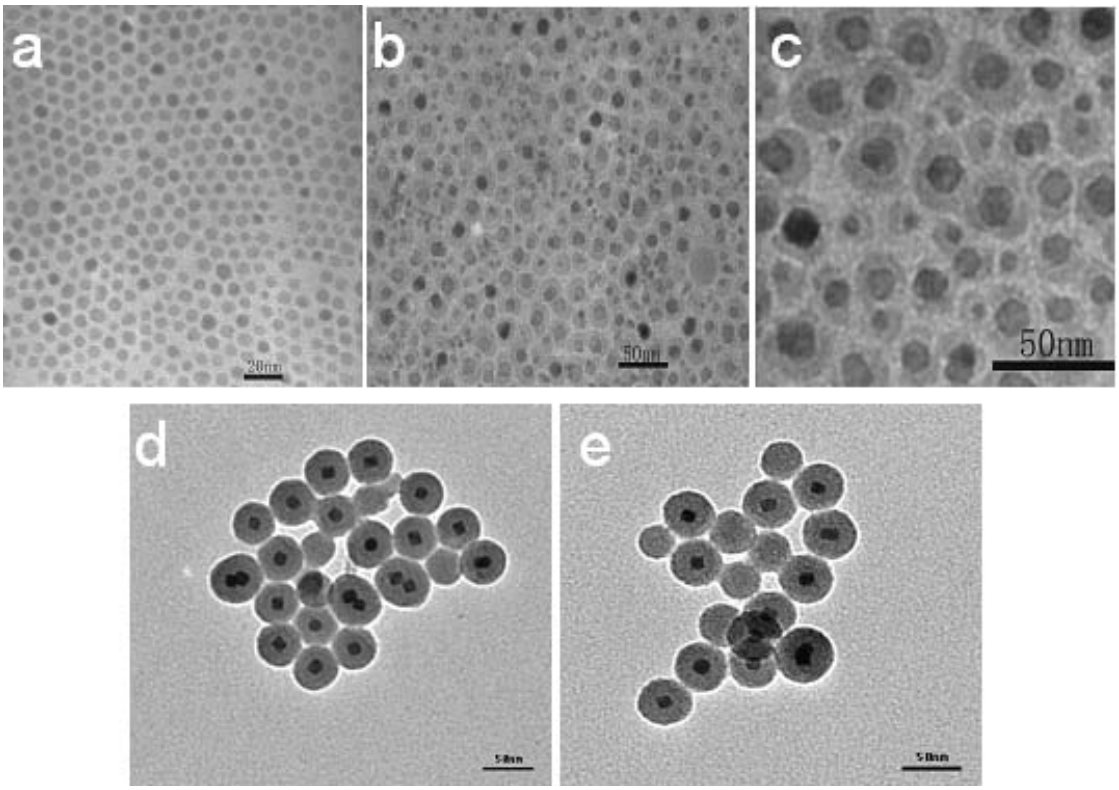

Figure 5.2. XRD pattern of (a) bare Fe_3O_4 nanoparticles; and (b)Fe_3O_4@SiO_2 nanocomposite. All the peaks are matched and only amorphous silica peak can be found in Fe_3O_4@SiO_2 pattern.

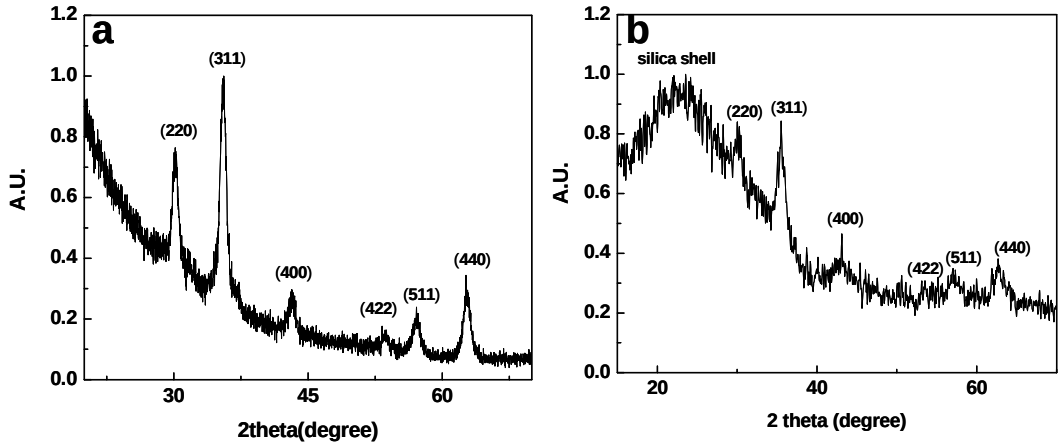

Figure 5.3. (a) Field-dependent magnetization of Fe_3O_4@SiO_2 at 300 K and 5 K; and (b) FC-ZFC curve for Fe_3O_4@SiO_2.

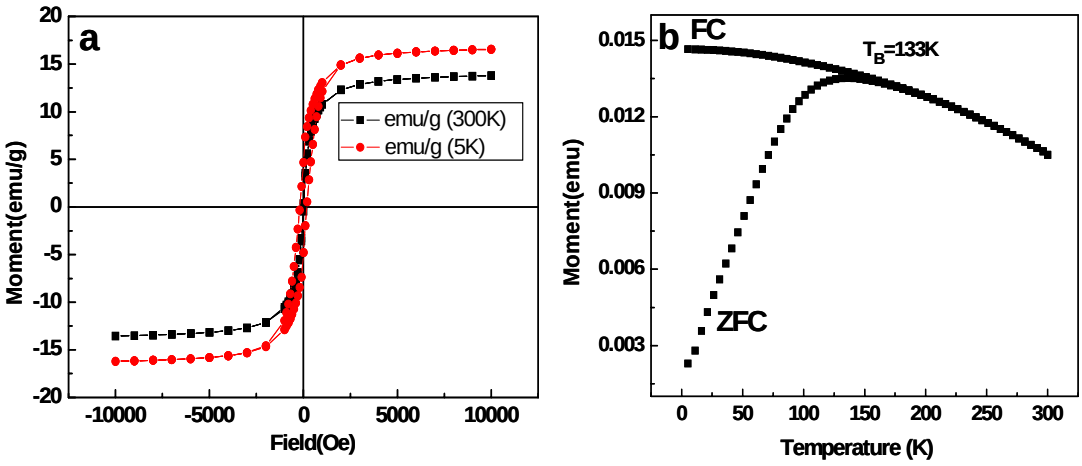

5.2.2 Synthesis of silica coated indium oxide nanoparticles

First, we synthesized In_2O_3 nanocrystals in degassed and high boiling point solvent hexadecane. Indium acetate, oleic acid, oleylamine and hexadecane were mixed and magnetically stirred under argon atmosphere. The mixture was heated to 110 ^{0}C for 30 minutes and then trimethylamine N-oxide was added to the mixture. The temperature of the reaction was increased to 160 ^{0}C for an additional 1 h. The mixture was quickly heated to reflux (~290 ^{0}C) for an additional 1 h. The bright brown-colored mixture was cooled to room temperature quickly and collected by centrifugation after adding a sufficient amount of ethanol. The precipitated particles were redispersed in hexane. The second step is to apply the silica shell by a modified water-in-oil microemulsion system at room temperature (Scheme 5.1). After transferring the In_2O_3 particles to cyclohexane dispersion, polyoxyethylene(5)nonylphenyl ether (Igepal CO-520) and ammonium hydroxide (28-30%) were added in a glass container under vigorous stirring and sonication. Thirty minutes after the light yellow transparent reverse microemulsion system formed, the specific amount of tetraethylorthosilicate (TEOS) was added and gently stirred for 48 h at room temperature to complete silica growth. The reaction mixture was precipitated and washed by acetone to remove the surfactant and any possible physically adsorbed molecules from the silica surface, and then collected by centrifugation. The resulting In_2O_3@SiO_2 particles can be redispersed in ethanol or water for future analysis. The interaction between surfactant (Igepal CO-520) and capping ligand (oleic acid) of the Indium oxide particles allows the hydrophobic particles to be encapsulated within the aqueous domain of the water-in-oil microemulsion. The surfactant Igepal CO-520 provided a bridge to connect the hydrophobic particles and

aqueous solution to form a composite structure with a water shell surrounding the surfactant containing the In_2O_3 particles. Furthermore, the ratio of the surfactant and ammonium hydroxide can be used to control the size of the microemulsion that will only allow one particle in each micelle.[29-46]

The samples were characterized by transmission electron microscopy (TEM) on a JEOL-2010 at an accelerating voltage of 200 kV. Figure 5.4a shows a representative TEM image of as-synthesized In_2O_3 particles that were stabilized by oleic acid. The particles were able to be dispersed very well in a hexane solution. The shape of the particles is close to the cubic and rhombic. The average size was around 15 nm. The high resolution TEM image in Figure 1b reveals the highly ordered fringes from the lattice structure of a typical crystal, which indicates the In_2O_3 nanoparticles possess high crystallinity without any dislocation or stacking faults. XRD data were collected with a Philips X'Pert Pro MPD system (equipped with a curved graphite single-crystal monochromater) using Cu Kα radiation. Figure 1c presents the XRD pattern of the In_2O_3 nanoparticles. All the detectable peaks can be indexed to body-center cubic In_2O_3 (JCPDS 00-006-0416), which confirmed the product was indeed In_2O_3 with a cubic structure.

Figure 5.5(a, b, c) are typical TEM images of silica coated indium oxide nanoparticles at different magnifications. Since the electron density of In_2O_3 is significantly larger than silica, we are able to observe the contrast difference between In_2O_3 and SiO_2. The dark

contrast in the center part of the particles corresponds to In_2O_3 core with a size of about 15 nm; and the light contrast on the edge of the particles shows the silica shell with a thickness of about 10 nm. The average size of the overall core-shell particles is about 35 nm. From figure 5.5a and 5.5b, the silica coating process is quite uniform. Almost all the In_2O_3 particles are coated by silica and no pure silica particles are formed; also the thickness of the silica shell is very similar between different particles. Figure 5.5c shows the detailed core-shell structure of a single In_2O_3@SiO_2 particle in the high resolution TEM image. Although the amorphous silica shell is coated, we are still able to observe the lattice fringes for the indium oxide core. The interplanar distance calculated from Figure 5.4b and 5.5c are both 2.9 Å, which corresponds to the lattice plane {222} for a cubic In_2O_3 crystal. This result indicates that the In_2O_3 particles are stable and inert during the silica coating process.

The composition of the In_2O_3@SiO_2 nanoparticles was estimated by energy- disperse X-Ray spectroscopy (EDS). Figure 5.6 shows the EDS analysis of the In_2O_3 core particles and In_2O_3@SiO_2 nanocomposites. It confirmed the presence of In in both bare In_2O_3 particles and core-shell nanocomposites. And the silica were only found in In_2O_3@SiO_2 nanocomposite (Cu, C were introduced from the TEM cupper grid).

The cubic In_2O_3 is known as an n-type semiconductor and the photoluminescence (PL) phenomenon for nanowires and nanoparticles has been reported as well. The normalized luminescence spectra of In_2O_3 nanoparticles before (black) and after silica (red) coating is

shown in figure 5.7 (PL was characterized on a Perkin-Elmer LS 55 luminescence spectrometer). As can be seen from the figure, the PL spectra show negligible changes in the peak emission wavelength following the silica coating process. The photophysical properties of In_2O_3 nanoparticles were almost not affected by the silica coating.

Figure 5.4. (a) TEM micrograph of In_2O_3 nanoparticles; (b) HRTEM image of a single In_2O_3 nanoparticle; (c) XRD pattern of In_2O_3 nanoparticles.

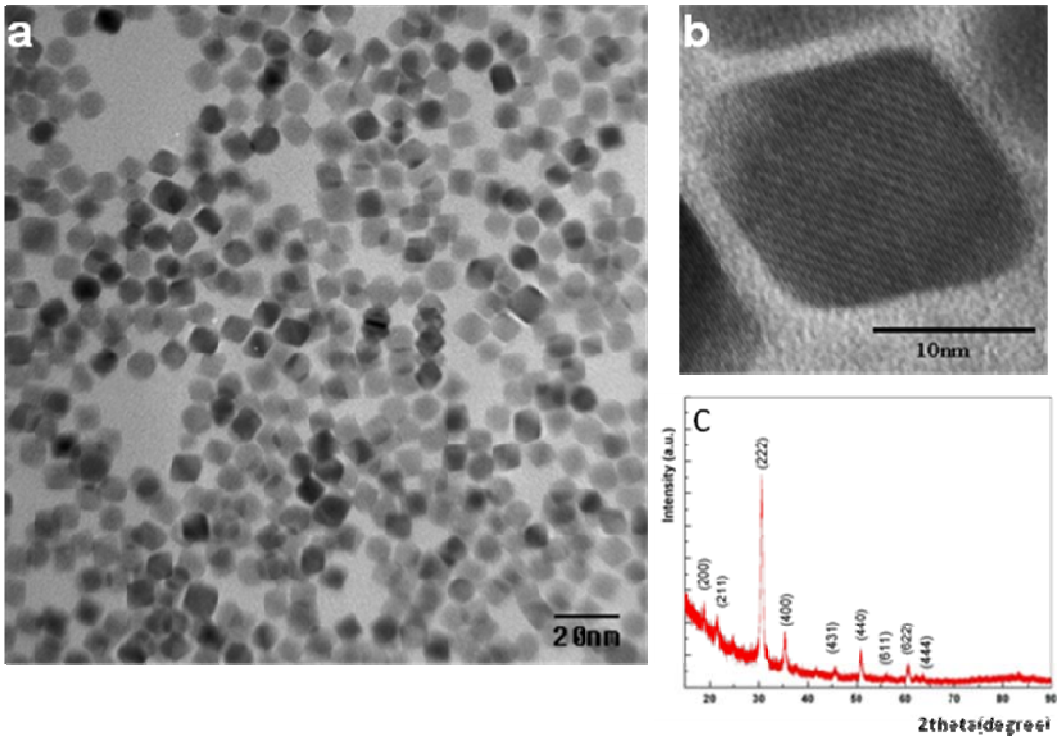

Figure 5.5 (a) TEM micrograph of core-shell structured In_2O_3@SiO_2 particles in low magnification; (b) TEM micrograph of core-shell structured In_2O_3@SiO_2 particles in high magnification; (c) HRTEM image of a single In_2O_3@SiO_2 core-shell structured particle.

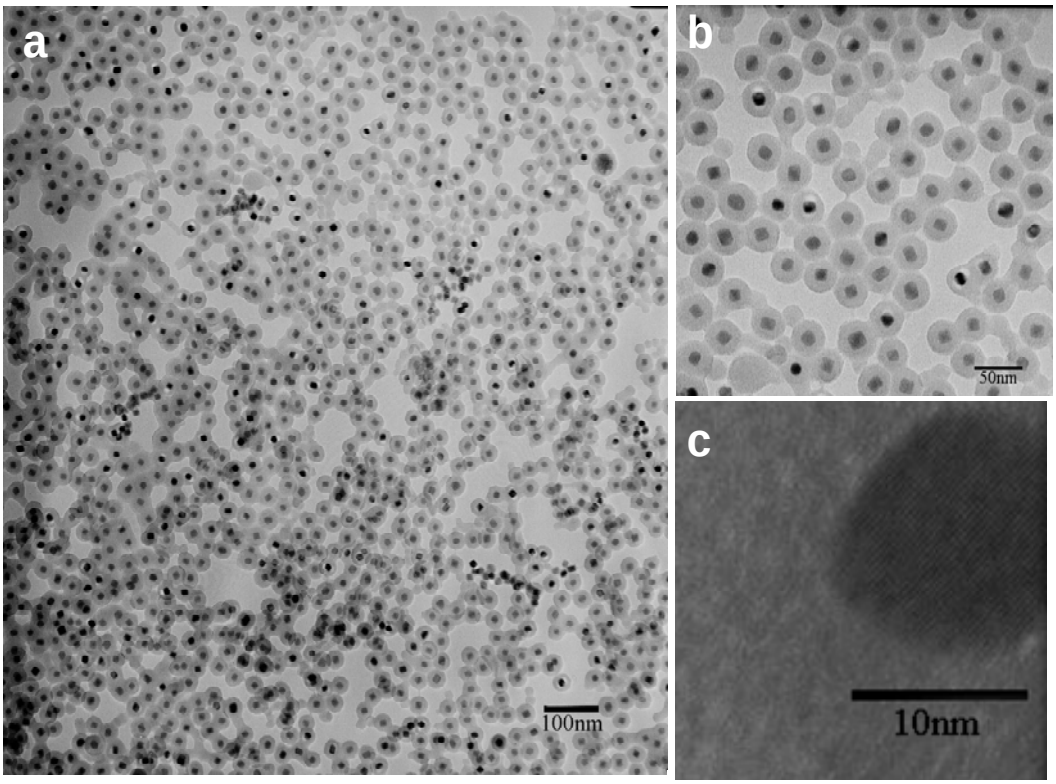

Figure 5.6. (a) EDS spectra of In_2O_3 nanoparticles; (b) EDS spectra of In_2O_3@SiO_2 nanoparticles. Only Si is present in silica coated composite.

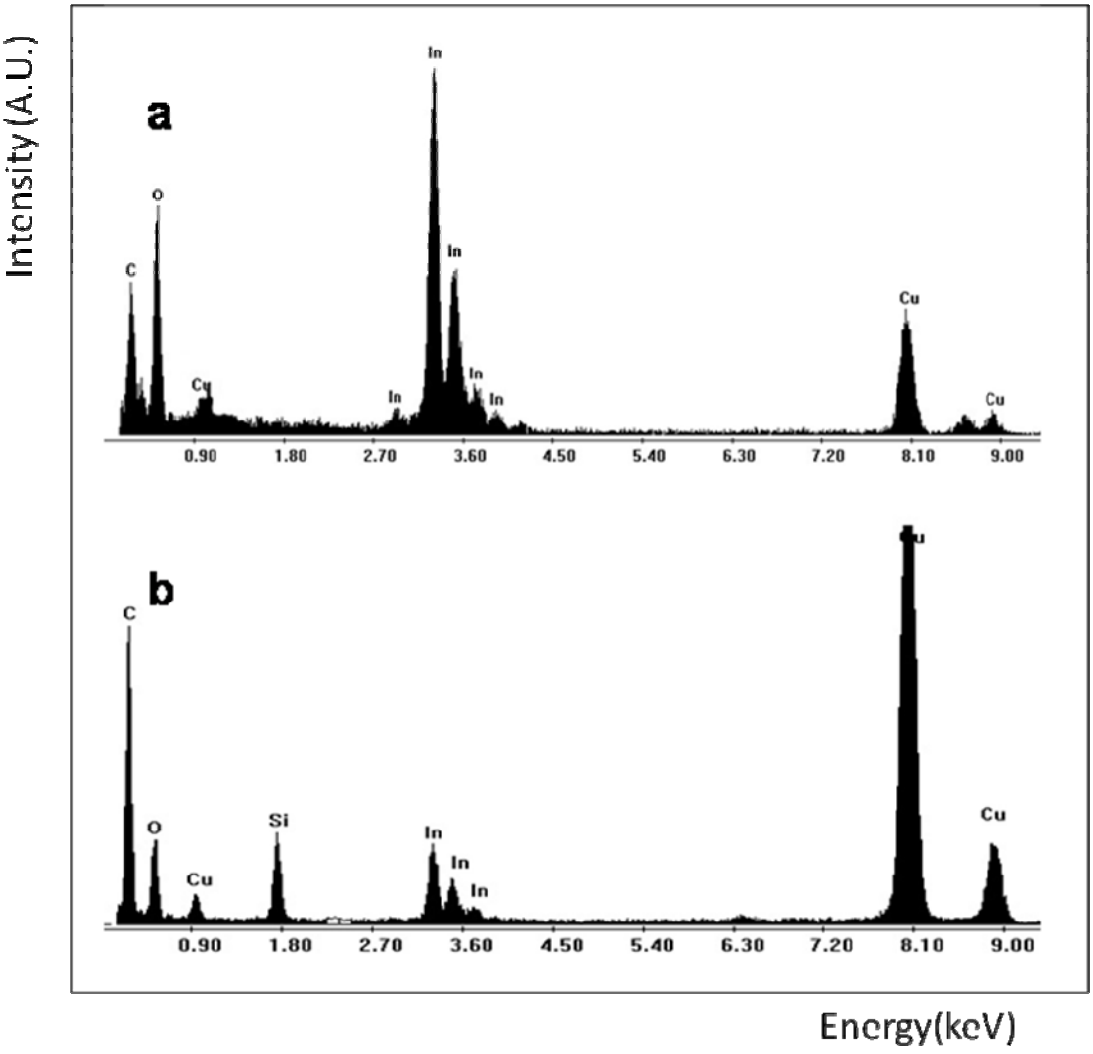

Figure 5.7. Normalized Photoluminescence spectra of bare In_2O_3 (black) and silica coated In_2O_3 (red). λex = 280nm. The emission peaks before and after coating are still in same wavelength which reveal the silica coating does not change the physical property.

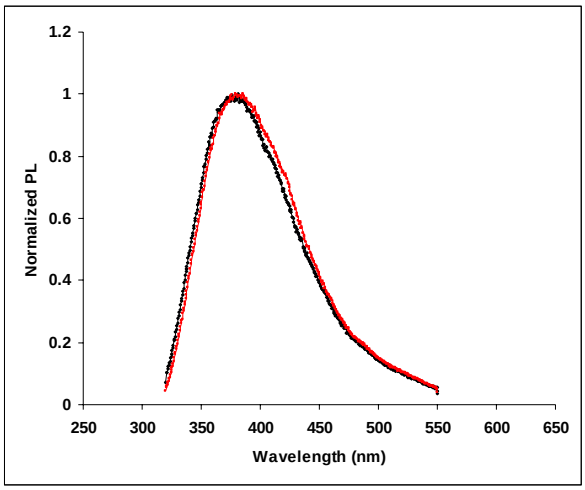

5.3 Discussion and Future work

5.3.1 Silica shell thickness tunable

The microemulsion system gives us the opportunity to tune the silica shell thickness based on the emulsion system principal. We can control the amount of water, the ration of Igepal CO-520 to water and amount of TEOS to get the specific shell thick we desire. To our knowledge, the shell thickness can be controlled ranging from 2nm to 100nm. This will bring us the advantage of designing the material architecture to satisfy the different applications.

5.3.2 Silica shell cross-linking

When in base condition, especially when the silica shells are getting thickness, the composite particles are trending to crosslink to form line or cluster. But we can avoid this situation by several methods. The most simple method is to add the extra amount of surfactant Igepa CO 520 as soon as the experiment are finished. With the assistance of the excessive surfactant, the final silica product will be kept in separate and avoid to aggregate.

5.3.3 Multiply core silica nanocomposite

When the silica shell gets thicker, the possibility to form multiply core composite are intensively increasing due to the space property. We can improve it by finding the optimum experimental condition, but it is difficult to avoid completely especially for the magnetic particles.

5.3.4 The relation of silica shell shape and core particle shape

Even though the silica coatings are spherical shape in most case, we still find the shape of silica shell is not spherical sometimes, which may be related with the non-spherical core particles. This phenomenon is still under investigated.

5.4 Conclusion

We have successfully synthesized the silica coated magnetite and indium oxide nanoparticles, respectively. The silica shells are uniform and robust to protect the core particle against acid, oxidation, decomposition and aggregation. Silica coating with our procedure is a “soft” technique, which will not change the structure and physical property of the core particles. Also silica has been proved to be able to manipulate with bio-labeling which could give our silica nanocomposite lots of applications. The tunable shell thickness will give us more flexibility to design our materials for different applications.

5.5 Reference

1. Meldrum, F. C.; Heywood, B. R.; Mann, S. *Science* **1992**, *257*, 522-523.
2. Tartaj, P.; Morales, M. P.; Gonzalez-Carreno, T.; Veintemills-Verdaguer, S.; Serna, C. T. *J. Magn. Magn. Mater*. **2005**, *290-291*, 28-34.
3. Willner, I.; Katz, E. *Angew. Chem., Int. Ed*., **2004**, *43*, 6042–6108.
4. Tanaka, T.; Matsunaga, T. *Anal. Chem.;* **2000**; 72*(15)*; 3518-3522.
5. Krizova, J.; Spanova, A.; Rittich, B.; Horak, D. *J. Chromatogr. A* **2005**, *1064*, 247-253.
6. Tartaj, P.; Serna, C. J. *J. Am. Chem. Soc*. **2003**, *125*, 15754-15755.
7. del Monte, F.; Morales, M. P.; Levy, D.; Fernandez, A.; Ocana, M.; Roig, A.; Molins, E.; O'Grady, K.; Serna, C. J. *Langmuir* **1997**, *13*, 3627-3634.
8. Matsura, V.; Guari, Y.; Larionova, J.; Guérin, C.; Caneschi, A.; Sangregorio, C.; Lancelle-Beltran, E. ; Mehdi, A;. Corriu, R. J. P. *J. Mater. Chem.*, **2004**, *14*, 3026-3033.
9. Deng, Y.; Wang, C.; Hu, J.; Yang, W.; Fu, S. *Colloids and Surfaces A: Physicochem. Eng. Aspects* **2005,** *262*, 87–93.
10. Lu, A.-H.; Li, W.-C.; Kiefer, A.; Schmidt, W.; Bill, E.; Fink, G.. Schuth, F. *J. Am. Chem. Soc.* **2004**, *126*, 8616-8617.
11. Santra, S.; Tapec, R.; Theodoropoulou, N.; Dobson, J.; Hebard, A.; Tan, W. *Langmuir;* **2001**; *17*(10); 2900-2906.
12. Yang, H.-H.; Zhang, S.-Q.; Chen, X.-L.; Zhuang, Z.-X.; Xu, J.-G.; Wang, X.-R. *Anal. Chem.***2004**; *76*(5); 1316-1321.
13. Im, S. H.; Herricks, T.; Lee, Y. and Xia, Y., *Chem. Phys. Lett.* **2005**, *401*, 19-23.

14. Haddad, P. S; Duarte, E. L; Baptista, M.S; Goya, G. F; Leite, C; Itri, R. *Prog. Colloid. Polym. Sci.*; **2004**; 128, 232-238.

15. Sun, S.; Zeng, H. *J. Am. Chem. Soc.* **2002**; *124*(28); 8204-8205.

16. Hyeon, T. *Chem. Commun.*, **2003**, 927-930.

17. Selvan, S. T.; Tan, T. T.; Ying, J. Y. *Advanced Materials* **2005**, *17(13)*, 1620-1625.

18. Kim, J.; Lee, J. E.; Lee, J.; Yu, J. H.; Kim, B. C.; An, K.; Hwang, Y.; Shin, C.-H.; Park, J.-G.; Kim, J.; Hyeon, T. *J. Am. Chem. Soc.;* **2006**; *128*(3); 688-689

19. Darbandi, M.; Lu, W.; Fang, J.; Nann, T. *Langmuir;* **2006**; *22*(9); 4371-4375.

20. Cheng, G.X.; Shen, F.; Yang, L.F.; Ma, L.R.; Tang, Y.; Yao, K.D.; Sun, P.C. *Mater.Chem. Phys*. **1998**, *56*, 97-101

21. Bae, D.S.; Han, K.S.; Adair, J.H. J. Mater. Chem., 2002, 12, 3117-3120

22. Tada, D. B.; Vono, L. L. R.; Duarte, E. L.; Itri, R.; Kiyohara, P. K.; Baptista, M. S.; Rossi, L. M. *Langmuir*; **2007**; 23(15); 8194-8199.

23. S.A. Empedocles, D. J. Norris and M. G. Bawendi, *Phys. Rev. Lett.* **1996**, *77*, 3873.

24. A. P. Alivisatos, *J. Phys. Chem*. **1996**,*100*, 13226.

25. C. B. Murray, D. J. Norris and M. G. Bawendi, *J. Am. Chem. Soc*. **1993**, *115*, 8706.

26. M. Jr. Bruchez, M. Moronne, P. Gin, S. Weiss and A. P. Alivisatos, *Science*, **1998**, *25*, 2013.

27. X. Gao, Y. Cui, R. M. Levenson, L. W. K. Chung and S. Nie, *Nature Biotech*. **2004**, *22*, 969.

28. L. Shi, V. De Paoli, N. Rosenzweig and Z. Rosenzweig, *J. Am. Chem. Soc.* **2006**, *128*, 10378.

29. D. Zhang, Z. Liu, C. Li, T. Tang, X. Liu, S. Han, B. Lei and C. Zhou, *Nano Letter* **2004**, *4*, 1919.

30. X. Li, M. W. Wanlass, T. A. Gessert, K. A. Emery and T. J. Coutts, *Applied Physics Letters* **1989**, *54*, 2674.

31. M. Liess, *Thin Solid Films* **2002**, *410*,183.

32. M. J. Zheng, L. D. Zhang, G. H. Li, X. Y. Zhang and X. F. Wang, *Applied Physics Letters,* **2001**, *79*, 839.

33. C. H. Liang, G. W. Meng, Y. Lei, F. Phillipp, and L. D. Zhang, *Advanced Materials* **2001**, *13*, 1330.

34. A. Murali, A. Barve, V. J. Leppert, S. H. Risbud, I. M. Kennedy and H. W. H. Lee, *Nano Letter* **2001**, *1*, 287.

35. Y. Zhao, Z. Zhang, Z. Wu and H. Dang, *Langmuir* **2004**, *20*, 27.

36. W. S. Seo, H. H. Jo, K. Lee and J. T. Park, *Advanced Materials*, **2003**, *15*, 795.

37. Y. Lei and W.-K. Chim, *J. Am. Chem. Soc*. **2005**, *127,* 1487.

38. Q. Liu, W. Lu, A. Ma,; J. Tang, J. Lin and J. Fang, *J. Am. Chem. Soc.* **2005**, *127*, 5276.

39. M. Darbandi, R.Thomann and T. Nann, *Chem. Mater*. **2005**, *17,* 5720.

40. S. T. Selvan, T. T. Tan and J. Y. Ying, *Advanced Materials* **2005**, *17*, 1620.

41. D. Gerion, F. Pinaud, S. C. Williams, W. J. Parak, D.Zanchet, S. Weiss and A. P. Alivisatos, *J. Phys. Chem. B.* **2001**, *105*, 8861.

42. C. Graf, D. L. J. Vossen, A. Imhof and A. van Blaaderen, *Langmuir* **2003**, *19*, 6693.

43. Z. Ye, M.Tan, G. Wang and J. Yuan, *Anal. Chem*. **2004**, *76*, 513.

44. Y. Lu, Y. Yin, Z. Y. Li and Y. Xia, *Nano Letter* **2002**, *2*, 785.

45. X. S. Peng, G. W. Meng, J. Zhang, X. F. Wang, Y. W. Wang, C. Z. Wang and L. D. Zhang, *J. Mater. Chem*. **2002**, *12*, 1602.

46. H. Cao, X. Qiu, Y. Liang and Q. Zhu, *Applied Physics Letters* **2003**, *83*, 761.

Chapter 6 Synthesis of Titania and polymer coated nanoparticles

6.1 Introduction

We have successfully coated the silica shell on metal oxide nanoparticles which has been discussed in previous chapter. And we would like to extend our coating technique to other materials such as titania and polymer because both materials are used widely for numerous applications.

6.1.1 Titanium Dioxide Coating

Since its commercial production in the early twentieth century, titanium dioxide has been widely used as a pigment and in sunscreens, paint, ointment, toothpaste, etc. Recently, enormous effeorts have been devoted to the research of TiO_2 material, which has led to many promising applications in areas ranging from photovolaics and photocatalysis to photo-electrochromics and sensors. These applications can be roughly divided into energy and environment categories, many of which depend not only on the properties of the TiO_2 itself but also on the modification of TiO_2 material and on the interactions of TiO_2 materials with the environment. An exponential grown of research activities has been seen in nanoscience and nanotechnology in the past decades. New physical and chemical properties emerge when the size of the material becomes smaller and smaller, and down to the nanometer scale. Properties also vary as the shapes of the shrinking nanomaterials change. As the most promising photocatalyst, TiO_2 materials are

expected to play an important role to helping solve many sevious environment and pollution challenges. TiO_2 also bears tremendous hope in helping ease the energy crisis through effective utilization of solar energy based on photovoltaic and water-splitting devices.

For the synthetic method for TiO_2 nanostructures, many different approaches have been developed to make TiO_2 particle, rod, wire, tube, opal and nanoporous structure such as sol-gel method, micelle and inverse micelle method, hydrothermal, solvothermal method, chemical vapor deposition, physical vapor deposition, electrodeposition, aerogels, sonochemical method and microwave method, etc. Each method has its own advantage and disadvantage. In this chapter, I will discuss some result of Titanium dioxide coated magnetite nanoparticles based on the reverse micelle method.[1-4]

6.1.2 Polymer Coating

The synthesis and processing of nanocomposite consisting of magnetic nanocrystal cores and organic polymer monolayer shells promises interesting technological appellations. In recent years, there has been increased interest in coating surfaces of nanoparticles with a thin shell material for various electronic and biomedical applications. Recently, polymeric shells have proven to be one of the best coating materials. Methods to coat a polymer shell with a controllable thickness on magnetic nanoparticles may aid in the development of ordered arrays of magnetic nanoparticles. The formation of polymeric shells is essential for biomedical applications of magnetic nanoparticles such as magnetic targeting drug delivery and magnetic resonance imaging contrast

enhancement. Also one of the most recent interests is the functionalizing the surface of magnetic nanoparticles for applications in biomedicine which require narrow size distribution or uniform monodispersed nanoparticles with desired chemical and biological surface functionalities. In such applications, the nanoparticles would benefit from having a shell structure to increase the mechanical stability, water solubility, and biocompatibility and prevent aggregation. Biocompatible polymer is proved to be one of the best coating materials due to its chemical stability and transparency. Recently many research efforts have been devoted to the preparation of monodispersed superparamagnetic nanoparticles, where polymers have been used in their surface modification. Among the various synthetic strategy of polymer coating, there are three major experimental routes to make polymer coated magnetic nanoparticles. First route is so-called one-pot synthesis which polymer is used as capping ligands to bind to the magnetic particles directly during the particles formation process.[10] The second route is based on the ligand exchange reaction between polymer and capping ligand on the surface of magnetic nanoparticles. Those two methods both use pre-made polymer for binding and attaching to the surface of magnetic particles. For the third experimental route the monomer is used as precursor and the polymerization process occurs on the surface of the magnetic particles. Dr Yang and his coworkers reported that the Fe_2O_3@polystyrene core-shell structure nanoparticles can be obtained by atom transfer radical polymerization (ATRP) method.[13] The key step of the synthesis is to apply the ligand exchange process with 2-bromo-2-methylpropionic acid (Br-MPA) to generate microinitiators on the surface of magnetic particles which can be further induced to form free radicals on the surface of magnetic particles to initiate the polymerization process on

the particle surface. But the polymer coating with ATRP approach cannot achieve large molecular weight product. In this chapter, we will report another synthetic strategy to make the polymerization process only occur surrounding the magnetic particles to form core-shell structure. Furthermore, we will discuss the magnetic property of the nanoparticles during the emulsion polymerization process.[5-12]

6.2 Experimental procedure

We first synthesize the core particle magnetite separately based on the method we discussed in previous chapter. Then we apply the titania or polymer coating in reverse microemulsion system. For titanium dioxide coating, it is very similar method with our silica coating procedure except by using titanium (IV) alkoxide as precursor. The resulting product is light-brown color and can be dispersed in ethanol solution. For the polymer coating, the experiment procedure is a little bit complicated due to the addition of the initiators. We will use PMMA coating as an example to show the typical polymer coating approach. After transferring the oleic acid stabilized magnetic particles to cyclohexane, the surfactant polyoxyethylene(5)nonylphenyl ether (Igepal CO-520) and specific amount of the initiator potassium persulfate aqueous solution were added to form a brown transparent microemulsion solution with the aid of a sonicator. Then, the monomer MMA was added and the solution was heated at 80^0C for 12h. The result product was collected by centrifuge and redispered in ethanol, producing a clear solution with brown color. With the similar synthetic route, we also coated poly-styrene on the surface of the magnetite particles.

6.3 Results and discussion

The general approach that was developed to synthesize titania and polymer- coated magnetite nanoparticles can be found in Scheme 6.1a.

In the case of titania coating, the representive TEM image shows the titania tiny particles formed surrounding the magnetite particles. The designed core-shell structure was not clearly observed instead of the very small titania particles formed instead. The possible reason for that might be the reaction rate. Because the titania precursor's hydrolysis rate is much faster than silica precursor. During the coating reaction, the titania form the nuclei process very quickly, and hydrolysis process happened in first a few second of the reaction, which cause the tiny titania particles formation. We tried to improve the hydrolysis result by decreasing the amount the water and using the lower temperature.

In the case of polymer coating, the clear core shell structure was showed even through the magnetic particle is somewhat aggregated. Figure 6.1A shows a representative TEM image of as-synthesized Fe_3O_4 magnetic particles which were stabilized by oleic acid and can be dispersed very well in non-polar solvent. The average size was around 10nm and the shape is close to spherical shape. And Figure 6.1B shows a typical TEM image of Fe_3O_4@PMMA magnetic nanocomposite dispersed in ethanol. Although the magnetic particles were partially aggregated during the process of the polymer coating, the polymer shell is readily apparent and the thickness of polymer shell is around 5~6nm.

The surfactant Igepal CO-520 played the important role to connect oleic acid capping magnetite particles and aqueous initiator solution. Igepal CO-520 is a type of

non-ionic surfactant which is consisted by the hydrophobic part and hydrophilic part. In the microemulsion system, the hydrophilic terminal of the Igepal CO-520 will attract the initiator ion of the aqueous solution and the hydrophobic terminal will be connected to the oleic acid stabilized magnetite particle. So the initiator is likely to be concentrated to the surface of magnetic particles with the aid of Igepal CO-520. Even though the monomer methyl methacrylate was dissolved in solvent cyclohexane, the polymerization reaction will occur only on the surface of magnetite particles.

The amount of reaction agents is another important parameter. The ratio of surfactant to water is a key to the micelles formation and their size and stability. It will allow us to control the micelles to contain only one particle inside, which lead to form the single core composite. The amount of the monomer will be used to control the shell thickness. Further study will be made to investigate the optimum condition to form the non-aggregated core-shell structure.

Scheme 6.1 Emulsion polymerization process on the surface of nanoparticles

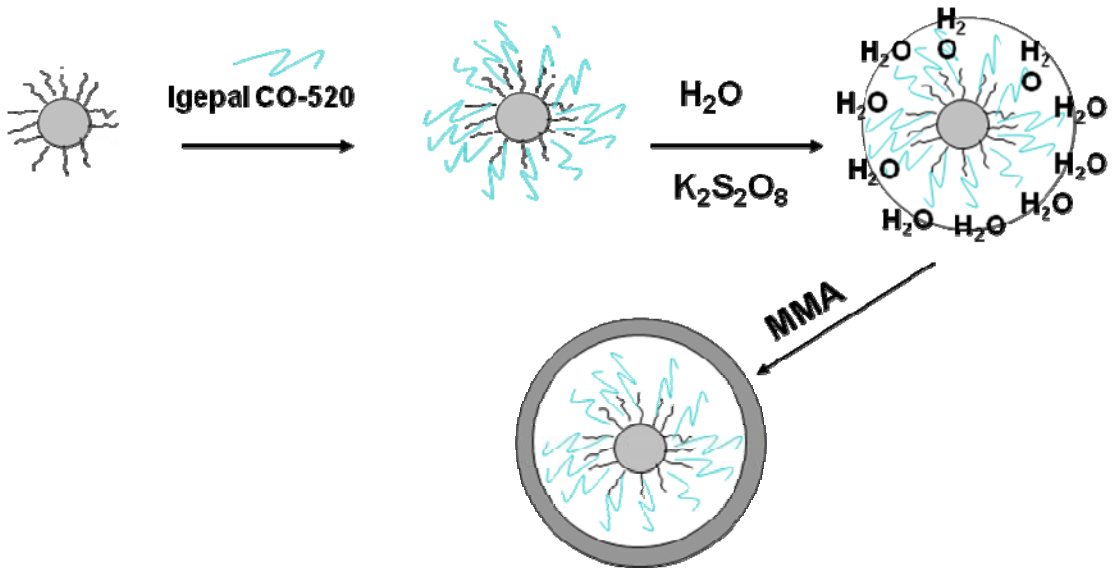

Figure 6.1 TEM micrograph of (A) as-synthesized Fe_3O_4 magnetic particles and (B) Fe_3O_4@PMMA nanoparticles.

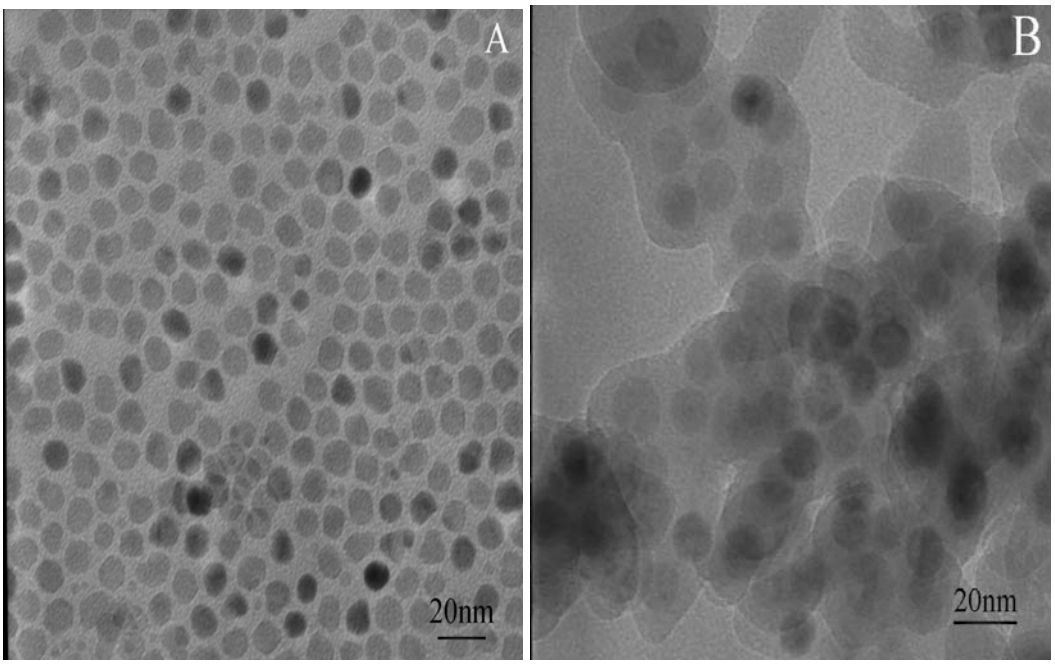

We also studied the polystyrene coated magnetite nanoparticles. With Polystyrene coated, the morphology of the composite seemed more uniform and the magnetic cores are not aggregated as PMMA coated composite. We think the aggregation of the core magnetite particles might be caused of the heat treatment. In the styrene polymerization process, we use the temperature 45^0C instead of 80^0C for PMMA, and the resulting products are clearly core shell without the severe aggregation. [13]

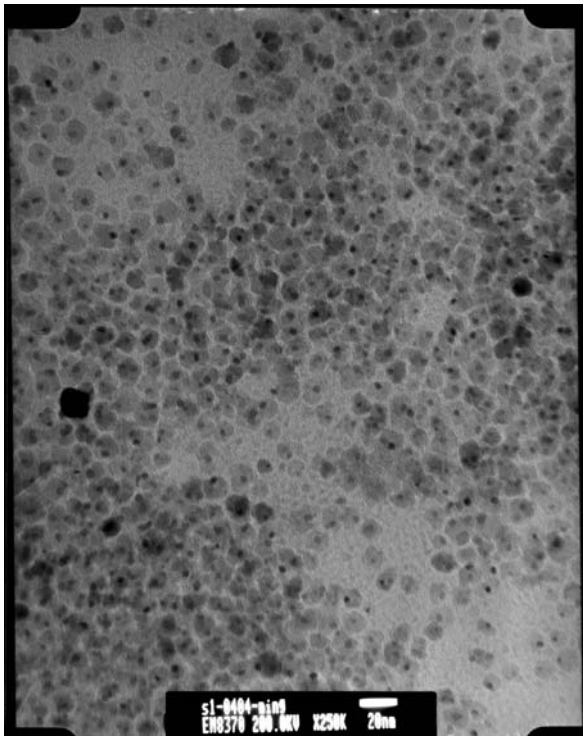

Figure 6.2 TEM micrograph of Fe_3O_4@PS nanoparticles. The magnetite particles of PS coating are much less aggegated comparing to PMMA coating.

6.4 Conclusion

We have successfully synthesized polymer-coated magnetic nanocomposite via a reverse micelles method and did some preliminary research on the titanium dioxide coating. And we also investigated the relationship of the experiment parameter and the resulting products.

6.5 Reference

1. Tartaj, P.; Serna, C. J. *J. Am. Chem. Soc*. **2003**, *125*, 15754-15755.
2. Tartaj, P.; Morales, M. P.; Gonzalez-Carreno, T.; Veintemills-Verdaguer, S.; Serna, C. T. *J. Magn. Magn. Mater*. **2005**, *290-291*, 28-34.
3. Willner, I.; Katz, E. *Angew. Chem., Int. Ed*., **2004**, *43*, 6042–6108.
4. Meldrum, F. C.; Heywood, B. R.; Mann, S. *Science* **1992**, *257*, 522-523.
5. Kim D.K., M. Mikhaylova, Y. Zhang & M. Muhammed, *Chem. Mater*. **2003**, *15*, 1617–1627.
6. Sun, S.; Zeng, H. *J. Am. Chem. Soc.* **2002**, *124*(28); 8204-8205.
7. Hyeon, T. *Chem. Commun.*, **2003**, 927-930.
8. Caruntu D., G. Caruntu, Y. Chen, G. Goloverda, C.J. O'Connor , V. Kolesnichenko, *Chem. Mater.* **2004**, *16*, 5527–5534.
9. Kang, N.; Perron, M.-E.; Prud'homme, R. E.; Zhang, Y.; Gaucher, G.; Leroux, J.-C. *Nano Lett.;* **2005**, *5(2);* 315-319.
10. Huang, X.; Brittain, W. J. *Macromolecules*; **2001**, *34(10);* 3255-3260.

11. Zhang, Q.; Xu, T.; Butterfield, D.; Misner, M. J.; Ryu, D. Y.; Emrick, T.; Russell, T. P. *Nano Lett.;* **2005**, *5(2),* 357-361.

12. Guo Q., S. Rahman, X. Teng & H.J. Yang. *J. Am. Chem. Soc*. **2003**, *125*, 630–631.

13. Wang, Y.; Teng, X.; Wang, J.-S.; Yang, H. *Nano Lett*.; **2003**, *3(6),* 789-793.

Chapter 7 Summary and Conclusions

This Ph.D. dissertation consists of two parts. In the first part, nonaqueous solution synthesis and characterization of crystalline metal oxide nanoparticles such as magnetite (Fe_3O_4), Indium oxide (In_2O_3), cobalt ferrite ($CoFe_2O_4$) and lithium cobalt oxide ($LiCoO_2$) are described. The second part of the dissertation focuses on the development of novel surface coating techniques to synthesize core-shell structure nanocomposites using some of those metal oxide nanoparticles as the core and silica, titania or polymer as shell via a modified microemulsion approach.

Magnetite (Fe_3O_4) nanoparticles were synthesized in high boiling point organic solvents involving the reaction between $Fe(acac)_3$ and 1,2-hexadecanediol. The size of those nanoparticles can be tuned from 4 nm to about 20 nm by the seed mediated growth approach (small particles treated as new nuclei to form larger particles). The small magnetite particles show spherical morphology in shape and the larger particles show hexagonal shape. We were also able to alter the particle shape transition producing magnetite particles with increasing size. This new discovery will lead us to continue our research on the mechanism of nanoparticle formation. With a similar synthetic approach, cobalt ferrites were synthesized successfully by using $Co(acac)_2$ and $Fe(acac)_3$ as the metal precursors instead of the single metal precursor $Fe(acac)_3$.

The Indium oxide (In_2O_3) nanoparticles were synthesized by a nonaqueous thermodecomposition approach with $In(ac)_3$ as the metal precursor. The size of In_2O_3 nanoparticles can be tuned from 8 nm to 20 nm with seed mediated growth and the shape

can be well controlled by adjusting the type and amount of the capping ligands and reaction conditions. The spherical and diamond shape nanoparticles were achieved, respectively. And in this thesis, we were the first to discover that the aggregation of small In_2O_3 particles will lead to form the larger diamond shape crystals. With the similar approach, the uniform cubic shape $LiCoO_2$ nanoparticles were first reported to be prepared by using Lithium acetate and Cobalt (III) acetate as metal precursors.

All of our particles are monodispersed and exhibit narrow particle size distribution, high crystallinity and high dispersibility in non-polar solvents. With the size selection technique, the different size particles were separated with a tight size distribution. Those uniform nanoparticles show unique physical properties and trend to form monodispersed self-assembled monolayers.

We also report the synthesis of the core-shell structure nanocomposites by using some of these nanoparticles as the core with silica, titania or polymer as the shell via a modified microemulsion approach. By using a microemulsion system, the core-shell structure silica coated iron oxide and indium oxide nanocomposites are successfully prepared. Furthermore, the thickness of the silica coating can be controlled from 2 nm to about 100 nm by adjusting the reaction agents of the micelle system. The silica coating process is a kind of "*soft*" process and the crystal structure and physical property of the core metal oxide nanoparticles remain the same during the silica coating.

We were the first to report the fabrication of ultra thin (~1-2 nm) silica coated magnetite with excellent magnetic properties. Due to the very thin silica shell, the saturation magnetization (M_S) of the Fe_3O_4@silica nanocomposite is around 15emu/g,

which is a significant improvement over the values previously reported in the literature (generally below 5emu/g). Compared to the recent silica coating techniques, our method is the only way to make the ultra thin silica layer down to ~1-2 nm. Our method is also a very versatile approach which can be used for silica coating of any stable nanoparticles with hydrophobic capping ligands on the surface.

Through an extension of our novel procedures we have also reported the titania and polymer coating preparation and characterization. We also reported the relationship between the reaction polymerization temperature and particle aggregation.

VITA

Ming Zhang was born on November 2nd, 1979 in Wuhu City, Anhui Province, P. R.China. He obtained his Bachelor's degree in polymer Science and engineering from University of Science and Technology of China in 2002. Also he earned his second Bachelor's degree in computer science at the same time. Then, in August 2002, he came to U.S.A and joined the chemistry department of the University of New Orleans. Later that year, he joined Advanced Materials Research Institute and Dr. Charles O'Connor's group and conducted his research in the field of nanomaterials under the guidance of Dr. O'Connor.